論文 / 著書情報
Article / Book Information

題目(和文)	
Title(English)	Novel Thermoplastic Elastomers by Reactive Blending of Thermoplastic and Rubber
著者(和文)	JANTANASAKULWONGK
Author(English)	KITTISAK yuingying
出典(和文)	学位:博士(工学), 学位授与機関:東京工業大学, 報告番号:甲第9280号, 授与年月日:2013年9月25日, 学位の種別:課程博士, 審査員:扇澤 敏明,鞠谷 雄士,塩谷 正俊,淺井 茂雄,松本 英俊
Citation(English)	Degree:Doctor (Engineering), Conferring organization: Tokyo Institute of Technology, Report number:甲第9280号, Conferred date:2013/9/25, Degree Type:Course doctor, Examiner:,,,,
学位種別(和文)	博士論文
Type(English)	Doctoral Thesis

Novel Thermoplastic Elastomers by Reactive Blending of Thermoplastic and Rubber

Kittisak Jantanasakulwong

Department of Organic and Polymeric Materials

Doctoral Thesis

2013

TOKYO INSTITUTE OF TECHNOLOGY

GRADUATE SCHOOL OF ENGINEERING

O-OKAYAMA (大岡山) CAMPUS.

Doctoral Thesis

Department of Organic and Polymeric Materials

Graduate School of Science and Engineering

Tokyo Institute of Technology

Contents

CHAPTER 6

General Conclusions

Acknowledgements

CHAPTER 1

General Introduction

Recently, thermoplastic elastomer (TPE) has attracted much attention because of its ease in melt processing and the advantage of reprocessability of used products. TPE exhibits both the processing characteristics of thermoplastics and the elastomeric properties like vulcanized rubber, and has been replacing vulcanized rubbers in some applications. Because of its ease in reprocessing, TPE is regarded as an environmentally friendly material compared to the vulcanized rubber. TPE has been widely used as a material for automobile, electrical products, packaging, medical products, etc. Thermoplastic vulcanizate (TPV) is a kind of TPE, which is made by a polymer blend consisting of both thermoplastic matrix and crosslinked rubber dispersed phase. To obtain the TPV with excellent properties, the rubber dispersed phase should be uniformly distributed and the particle size should be fine. Moreover, tensile properties of TPE should show low modulus, high tensile strength at break, high elongation at break and excellent strain recovery like a vulcanized rubber.

The preparation of TPE by melt-blending of a thermoplastic and a rubber is the simple and cost-effective method. Nevertheless, most of polymer pairs are intrinsically immiscible. In some cases, the blends show poor mechanical properties when the blend morphology is coarse and the interfacial adhesion between the matrix and the dispersed

phases is low.[1] Reactive blending is one of the effective techniques to induce higher compatibility between two immiscible polymers. By addition of a suitable chemical, interfacial tension between two phases during melt-mixing process is lowered and it leads to finer morphology and improvement of the interfacial adhesion. The addition of some chemicals to the blend has been studied extensively in the area of reactive blending. For example, hexamethylenediamine carbamate,[2] N,N'-m-phenylene-bis-maleimide[3] and dicumyl peroxide[4,5] have been used as the chemicals. In addition, the rubbers grafted with various reactive groups, such as maleic anhydride,[1,6] glycidyl methacrylate[7] and allyl (3-isocyanate-4-tolyl)[7], have been also used to compatibilize the thermoplastic and the rubber. Several reports employed ethylene-methacrylic acid ionomer as a compatibilizer to improve the interfacial adhesion between two component polymers in a blends[8-9].

As a rubber material in TPV, various types of rubber such as ethylene-propylene-diene terpolymer[10-12], ethylene-propylene rubber[12-14], and natural rubbers[15-18] have been widely used. Many kinds of thermoplastics were used to prepare TPEs such as polypropylene,[19] poly(ethylene terephthalate),[20] poly(butylene terephthalate)[7] and poly(vinylidene difluoride).[21] The idea of high thermal- and oil-resistant TPE also motivated some researchers to investigate, and it has been studied by using a plastic of high melting point such as polyamide.[22-23]

Most of the commercial polymers made from petroleum are non-biodegradable and non-biobased, and then the applications consuming such polymers have led to the problem of solid-waste management and limited petroleum resources. To overcome this problem, biodegradable and bio-based plastics have attracted much attention in recent

years. They are the environmentally friendly polymers because of its renewability and biodegradability. The combinations of reprocessability, elasticity, environmental friendliness and excellent mechanical properties have motivated some researchers to develop biodegradable TPEs. They have tried to develop TPEs by biodegradable plastics such as polycaprolactone (PCL)[5] and poly(lactic acid) (PLA).[24-26] However, as for my knowledge, TPEs based on a biodegradable thermoplastic blend with excellent mechanical properties have not been achieved so far.

Objective of this thesis

The aim of this thesis is to develop novel TPEs by reactive blending of a thermoplastic with a rubber in various kinds of reactive blending. The mechanical properties, thermal properties, rheological property, morphology and reaction of the TPEs were investigated.

The following are of particular interest:

I) To develop novel TPE based on biodegradable polymer blend.

II) To investigate effect of ethylene-acrylic acid ionomer as physical crosslinking agent or a compatibilizer on mechanical properties.

Individual investigations performed in this thesis are as follows:

(i) to investigate effect of annealing process on reaction-properties relationship of poly(butylene succinate) blended with maleic anhydride grafted rubbers.

(ii) to characterize compatibility and mechanical properties of poly(butylene succinate) and acrylic rubber blends by addition of dicumyl peroxide or poly[methylene (phenylene isocyanate)].

(iii) to investigate reaction-properties relationship of poly(lactic acid) and acrylic rubber blends with neutralized ionomer compatibilizer.

(iv) to study effect of neutralized ionomer as Crosslinking agent in the ternary blends of polyamide, maleic anhydride grafted ethylene-1-butene copolymer and ionomer.

REFERENCES

1. Chang, H. H.; Chau, H. W.; Chin, I. L.; Yu, D.L. *Polymer* **2008**, 49, 3902.
2. Li, Y.; Oono, Y.; Kadowaki, Y.; Inoue, T.; Nakayama, K.; Shimizu, H. *Macromolecules* **2006**, 39, 4195.
3. Bluma, G.S.; Marlucy, D.O.; Domenica, M.; Alex, S.S.; Raquel, S.M. *J. Appl. Polym. Sci.* **2008**, 110, 3566.
4. Tasdemir, M. and Topsakaloglu, M. *Polym. Mater.* **2006**, 55, 1065.
5. Mishra, J.K.; Chang, Y.K.; Kim, D.K. *Mater. Lett.* **2007**, 61, 3551.
6. Nakason, C.; Saiwaree S.; Kaesaman A. *Polym. Test.* **2006**, 25, 656.
7. Shi, Q.; Stagnaro, P.; Cai, C. L.; Yin, J. H.; Costa, G.; Turturro, A. *J. Appl.Polym. Sci.* **2008**, 110, 3963.
8. Lui, H.; Chen, F.; Lui, B.; Estep,G.; Zhang, J. *Macromolecules* **2010**, 43, 6058.
9. Lui, H.; Song, W.; Chen, F.; Guo, L.; Zhang, J. *Macromolecules* **2011**, 44, 1513.

10. Wu, C.J; Kuo, J.F.; Chen, C.Y.; Woo, E. *J. Appl. Polym. Sci.* **1994**, 52, 1695.
11. Hwang, C.I.; Park, O.O. *Polym. J.* **1995**, 27, 232.
12. Kunori, T.; Geil, P.H. *J. Macromol. Sci., Phys.* **1980**, B18(1), 135.
13. Lin, Q.; Yee, A.F. *J. Mater. Sci.* **1997**, 32, 3961.
14. Kil, S.B.; Park, O.O.; Yoon, K.H. *J. Appl. Polym. Sci.* **1999**, 73, 2123.
15. Tanrattanakul, V.; Kosonmetee, K; Laokijcharoen, P. *J. Appl. Polym. Sci.* **2009**, 112, 3267.
16. Mousa, A.; Ishiaku, U.S.; Ishak, Z. A. M. *J. Appl. Polym. Sci.* **1998**, 69, 1357.
17. Mishra, J. K.; Chang, Y. W.; Kim, D. K. *Mater. Lett.* **2007**, 61, 3551
18. Kim, J. K. *J. Appl. Polym. Sci.* **1996**, 61, 431.
19. Roy, M. A. I.; Martin, V. D.; Anne, B. S.; Johannes, G.P. *Soft Matter.* **2010**, 6, 1758.
20. Jha, A.; Bhowmick, A. k. *Polymer* **1996**, 4337.
21. Li, Y.; Kadowaki, Y.; Inoue, T.; Nakayama, K; Shimizu, H. *Macromolecules* **2006**, 39, 4195.
22. Jha, A.; Bhowmick, A. k. *Rubber Chem. Technol*., **1997**, 70, 798.
23. Jha, A.; Bhowmick, A. k.; Fujitsuka, R.; Inoue, T. *J. Adhesion Sci. Technol.* **1999**, 13, 649.
24. Kim, J.H.; Lee, J.H. *Polymer* **2002**, 34, 203.
25. Ishida, S.; Nagasaki, R.; Chino, K.; Dong, T.; Inoue, Y. *J. Appl. Polym. Sci.* **2009**, 113, 558.

26. Wanamaker, C. L.; Bluemle, M. J.; Pitet, L. M.; O'Leary, L. E.; Tolman, W. B.; Hillmyer, M. A. *Biomacromolecules* **2009**, 10, 2904.

CHAPTER 2

Thermoplastic Elastomer by Reactive Blending of Poly(butylene succinate) with Ethylene-Propylene-Diene Terpolymer and Ethylene-1-Butene Rubbers

2.1 INTRODUCTION

Thermoplastic vulcanizate (TPV) is a kind of thermoplastic Elastomer (TPE), and consisting of cross-linked rubber particles dispersed in thermoplastic matrix, and then it is reprocessable at the high temperature. To induce the crosslinking reaction in the rubber phase, chemicals such as dicumyl peroxide[1-3] as initiator of the reaction and hexamethylenediamine carbamate[4,5], phenolic resin[6] and tin chloride[6] as crosslinking agent have been used to additive to the blend. Moreover, to improve the compatibility between the rubber and the thermoplastic through interfacial reactions, chemicals such as dibutyl tin oxide[7] and dibutyltin dilaurate[8] as catalyst for transesterification, N,N'-m-phenylene-bis-maleimide[9] as coupling agent and hexamethylenediamine carbamate[7].

A rubber material grafted with a reactive group which can react with the thermoplastic matrix phase, has also been used to induce the interfacial reaction. Glycidyl methacrylate,[10] allyl(3-isocyanate-4-tolyl) carbamate[10] and maleic anhydride

(MAH)[11-13] are some examples of the grafted reactive groups on rubbers. Generally, MAH is grafted on to rubber in molten state.[13] However, MAH has low reactivity and then it is difficult to generate free radicals on MAH.[14-16] Alternatively, MAH can also be grafted onto a rubber by dissolving the rubber and MAH in a solvent with addition of peroxide for generating active sites.[12,13] Furthermore, many rubbers have also been grafted with MAH such as ethylene-propylene-diene terpolymer (EPDM),[17] ethylene-propylene rubber[18,19] and natural rubber.[20,21] As for MAH, it has also been grafted onto various copolymers[18-27] and thermoplastic materials such as ethylene vinyl-acetate copolymer,[22] polyethylene[28,29] and polypropylene.[23,30] The polymer blending with MAH grafted copolymer have been studied by many researchers.[11,13,18,20,28,30]

A biodegradable or a bio-based polymer, which is produced from renewable sources, is a promising candidate for an environmentally friendly material. Therefore, TPV prepared by a biodegradable polymer is also environmentally friendly material because it has combinated advantages of reprocessability and biodegradability. Nevertheless, not many studies have been reported on TPV using biodegradable polymers.[1,31,32] Among the several biodegradable or biobased polymers, poly(L-lactic acid) and polycaprolactone have been used to develop new TPV. However, as for my knowledge, TPV consisting of a biodegradable polymer with excellent properties have not been achieved so far.

Poly(butylene succinate) (PBS) is a biodegradable polymer and its mechanical properties are similar to polypropylene.[33] Scheme 2.1 is the chemical structure of PBS. Although PBS has been produced from petroleum-based 1,4-butanediol and petroleum-based succinic acid, completely bio-based PBS made from bio-based renewable

resources has also been developed and will be soon available.[34,35] Therefore, PBS will be a suitable material as a thermoplastic matrix polymer for TPV.

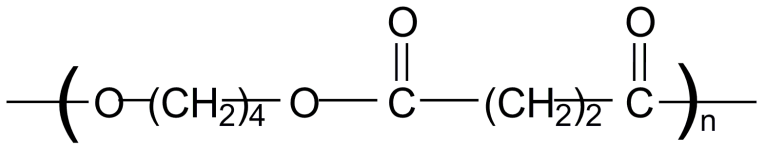

SCHEME 2.1 Chemical structure of PBS

2.1.1 Objective of this Chapter

In this chapter, novel TPV and TPE were developed by melt-blending of PBS with maleic anhydride grafted ethylene-propylene-diene terpolymer (EPDM-*g*-MAH) or maleic anhydride grafted ethylene-1-butene copolymer (EB-*g*-MAH). EPDM and EB are selected because these rubbers are valuable for their excellent resistance to heat, oxidation, ozone and weather aging due to their stable, saturated polymer backbone structure. The interest in this chapter was to observe effect of annealing process to improve reaction and mechanical properties of the blends. The relationship of their morphology, properties and reaction were investigated.

2.2 EXPERIMENTAL

2.2.1 Materials

PBS with a trade name of Bionolle was kindly provided by Showa HighPolymer Co., Ltd., of which the melting point is 115 ^{o}C and the melt flow index is 3.7 g/10 min at 190 ^{o}C. Maleic anhydride grafted ethylene-propylene-diene terpolymer (EPDM-*g*-MAH) (MAH content = 1 wt%, ethylidenenorbornene (ENB) content = 8.1 wt% and ethylene content = 52 wt%) was kindly supplied by Mitsubishi Chemical Corp., and maleic anhydride grafted ethylene-1-butene copolymer (EB-*g*-MAH) (MAH content = 1 wt% and 1-butene content = 20 wt%) was supplied by Mitsui Chemicals Inc. The chemical structures of EPDM-*g*-MAH and EB-*g*-MAH are presented in scheme 2.2 and 2.3 respectively.

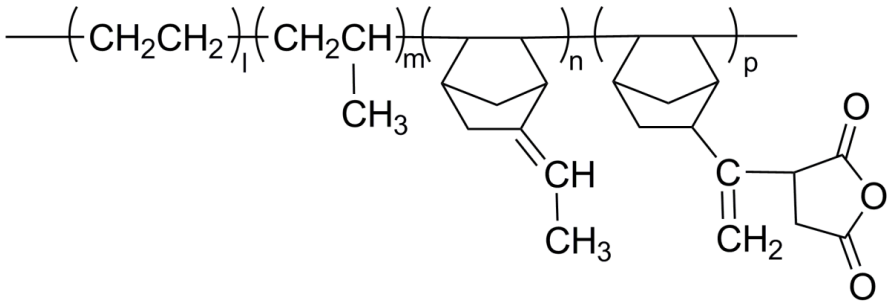

SCHEME 2.2 Chemical structure of EPDM-*g*-MAH

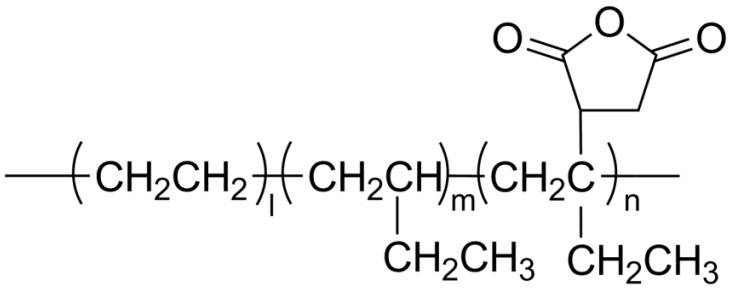

SCHEME 2.3 Chemical structure of EB-*g*-MAH

2.2.2 Samples Preparation

PBS was blended with one of the two kinds of rubbers, EPDM-*g*-MAH and EB-*g*-MAH respectively by melt-mixing in compositions of 40/60 at 160°C. The sample was mixed at the rotation speed of 100 rpm using a small-scale mixer (Mini-Max Molder, Model CS-183MM-065, Custom Scientific Instruments Inc.).

2.2.3 Measurements

2.2.3.1 Phase Determination

The blended samples (0.01 g) were immersed in 1 ml of toluene at room temperature for at least 24 h. Toluene is good solvent for EPDM and EB rubbers, while not for PBS. The components of matrix and the dispersed phase were checked from the residual component of the solution.

2.2.3.2 Tensile Properties Measurements

The dumbbell-shaped samples for the tensile test were prepared by compression molding. The gage length, width and thickness of the sample were 10 mm, 2 mm and

0.5 mm respectively. Tensile properties of the blends were measured by using tensile tester (Tensilon UTM-II-20, Orientec Co., Ltd) at room temperature with crosshead speed of 10 mm/min. The strain recovery test was also performed. After the preset strain of 100% was attained, the crosshead was returned to the original position at the same speed.

2.2.3.3 Scanning Electron Microscopy (SEM)

SEM (SM-200, Topcon Corp.) was used to investigate the morphology of the blends. The samples were broken in liquid nitrogen, and then the fracture surface of the samples was sputter-coated with gold, and the morphology was observed with an acceleration voltage of 10 kV.

2.2.3.4 Differencial Scanning Calorimetry (DSC)

Thermal behaviors of samples were measured by DSC (DSC6200, Seiko Instruments Inc.). A sample in an aluminum pan was heated from -100 to 150 ^{o}C under nitrogen gas flow at heating rate of 10 ^{o}C/min.

2.2.3.5 Fourier Transform Infrared Spectroscopy (FT-IR)

The samples were measured by FT-IR (FT/IR-480plus, Jasco Corp.). Films of samples were prepared by hot-press molding. The IR spectra were recorded in the range of 600 to 4000 cm^{-1} with a resolution of 4 cm^{-1}.

2.2.3.6 Degree of Cross-link Measurement

The samples (0.5 g) covered by nickel net were dissolved in chloroform at 25 ^{o}C for 24 h, and then the residual samples in the nickel net were dried at 60 ^{o}C for 24 h in order to remove the solvent. The gel percentage was calculated by Eq 1.

$$\text{Gel (\%)} = \frac{W_d - W_n}{W_o} \text{ x } 100 \quad (1)$$

Where W_d, W_n and W_o are the weight of the dried sample with nickel net after dissolution, the weight of the nickel net, and the initial weight of the sample, respectively.

2.3 RESULTS AND DISCUSSION

2.3.1 Phase Determination

Because the matrix phase of the blend should be a thermoplastic in TPE prepared by polymer blending, the component of the matrix phase was checked by dissolving the blend into a solvent. Figure 2.1 shows a picture of the immersed rubbers, PBS and the blended samples in toluene for 24 h. EPDM-*g*-MAH and EB-*g*-MAH completely dissolved into toluene [Figure 2.1(a) and (b)], while PBS was insoluble [Figure 2.1(c)]. Both PBS/EPDM-*g*-MAH and PBS/EB-*g*-MAH blends were also insoluble in toluene, and the shape of the samples did not change [Figure 2.1(d) and (e)]. If the matrix had been the rubber, the uncrosslinked rubber matrix had dissolved or the crosslinked rubber

had swollen to form a gel in toluene. These behaviors were not observed in both blends. Moreover it was also confirmed that the sample was reprocessable by melting. From the facts, it was suggested that the blend did not consist of crosslinked rubber matrix but of PBS matrix phase. The result shown in Figure 2.1(a)-(e) indicated that the morphology of these blends probably is co-continuous or sea-island structure with rubber dispersed phase and PBS matrix phase.

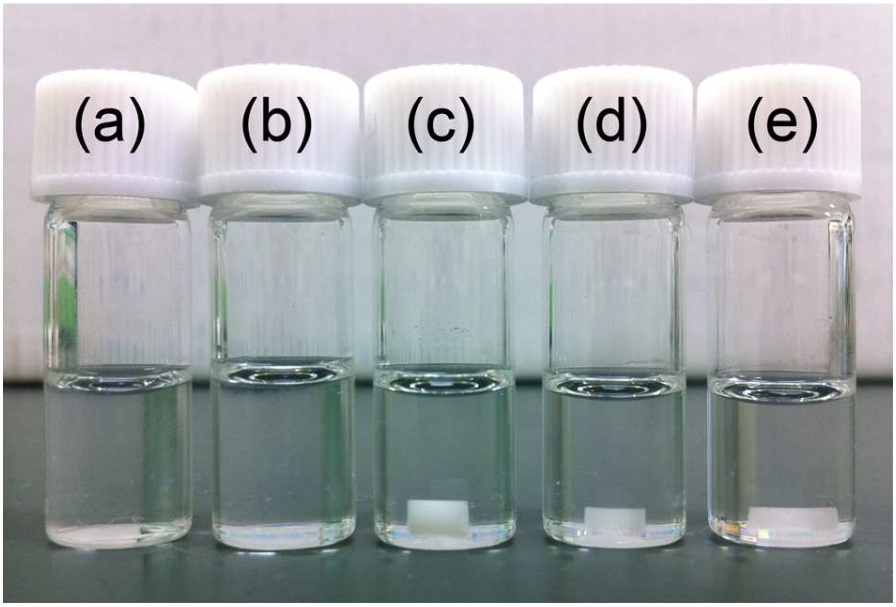

FIGURE 2.1 Picture of (a) EPDM-*g*-MAH, (b) EB-*g*-MAH, (c) PBS, (d) PBS/EPDM-*g*-MAH and (e) PBS/EB-*g*-MAH blends immersed into toluene at 25 ^{o}C for 24 h.

2.3.2 Morphology

PBS/EPDM-*g*-MAH and PBS/EB-*g*-MAH blends showed finer morphology, while PBS/EPDM and PBS/EB blends without MAH showed larger dispersed phase. Figure 2.2 shows the SEM fracture surface images of PBS/EPDM-*g*-MAH and PBS/EB-*g*-MAH blends. The images of both blends showed the sea-island phase separated structures. Considering the result of the phase determination experiment, it was confirmed that in both blends the rubber particles were dispersed in PBS matrix. EB-*g*-MAH rubber particle was much smaller than EPDM-*g*-MAH. It was suggested that the EB-*g*-MAH was more compatible with PBS than EPDM-*g*-MAH. The holes observed in the PBS/EPDM-*g*-MAH blend were due to the removal of some rubber particles from the fracture surface during cracking. It might be attributed to low interfacial adhesion between the PBS matrix and the rubber dispersed phase.

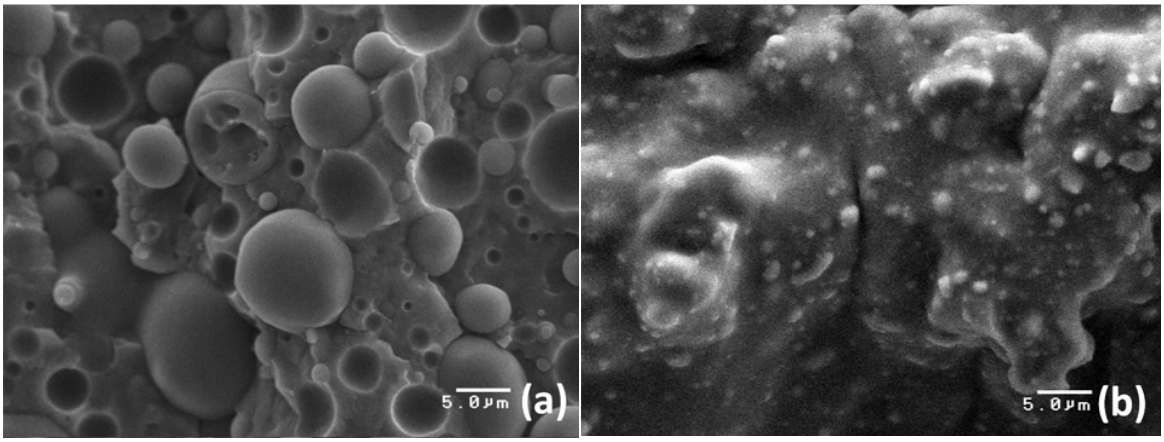

FIGURE 2.2 SEM images of fracture surface of (a) PBS/EPDM-*g*-MAH and (b) PBS/EB-*g*-MAH blends.

2.3.3 Mechanical Properties

Figure 2.3 shows the stress-strain curves of PBS, PBS/EPDM-*g*-MAH and PBS/EB-*g*-MAH blends. PBS showed high modulus, tensile strength and elongation at break, while PBS blends with EPDM-*g*-MAH and EB-*g*-MAH showed lower moduli and tensile strengths than neat PBS. Figure 2.4 shows the strain recovery curves of PBS, PBS/EPDM-*g*-MAH and PBS/EB-*g*-MAH blends. Both blends showed more superior strain recovery (～40% and ～70% respectively) than neat PBS (～20%).

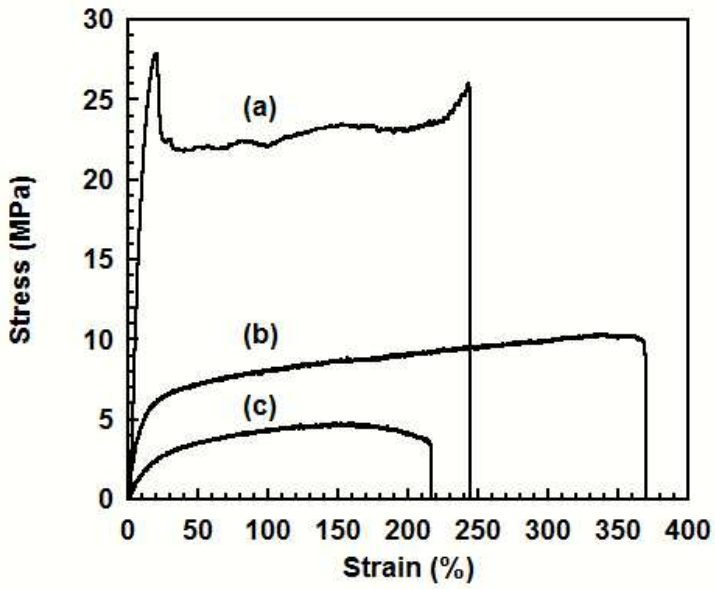

FIGURE 2.3 Stress-strain curves of (a) PBS, (b) PBS/EPDM-*g*-MAH and (c) PBS/EB-*g*-MAH blends.

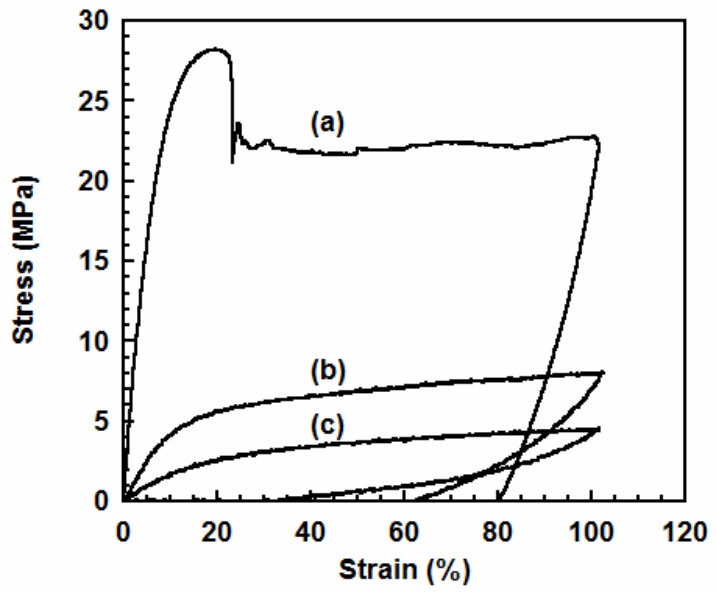

FIGURE 2.4 Strain recovery curves for (a) PBS, (b) PBS/EPDM-*g*-MAH and (c) PBS/EB-*g*-MAH blends.

2.3.4 Influence of Annealing on Mechanical Properties

From SEM images shown in Figure 2.2, the removal of rubber particles were observed, and this indicates the low interfacial adhesion between thermoplastic matrix phase and rubber dispersed phase. It was expected that annealing process at high temperature would increase the interfacial adhesion. However, the higher annealing temperature than 170 ^{o}C may induce thermal decomposition of PBS. Therefore, the blends were annealed at 170^{o}C for 0, 10, 30 and 60 min to improve the interfacial adhesion where the interfacial reaction was expected to proceed, and mechanical properties were analyzed by tensile test. Figure 2.5 shows the stress-strain curves of annealed PBS/EPDM-*g*-MAH and PBS/EB-*g*-MAH blends of different annealing times. PBS/EB-*g*-MAH blend showed lower tensile strength, elongation at break and modulus

than PBS/EPDM-*g*-MAH blend. Tensile strength and elongation at break of both blends increased with increasing annealing time, and tensile strength extremely increased in PBS/EPDM-*g*-MAH. The annealing effect on strain recovery of PBS/EB-*g*-MAH and PBS/EPDM-*g*-MAH blends is shown in Figure 2.6. Both blends with annealing showed the improvement in strain recovery of about 10%. The samples after measurement were retained at room temperature for one week, and then PBS/EB-*g*-MAH sample showed a slow recovery to 90%. Moreover, both PBS/EPDM-*g*-MAH and PBS/EB-*g*-MAH blends annealed at 170 ^{o}C for 60 min was reprocessable by melting. The excellent strain recovery of PBS/EB-*g*-MAH blend with annealing was due to the consequence of (*i*) the better elasticity of EB rubber, and (*ii*) small size of rubber particles, and it also may be due to (*iii*) the increased interfacial adhesion by the annealing. The mechanism of elastic recovery in TPE has been explained by the existence of non-yielded ligament of plastic matrix phase between rubber particles in the stretching direction even at highly deformed states at which almost the matrix is yielded by stress concentration, and it acts as joint region for interconnecting rubber particles.[36] The interfacial adhesion between the two phases and the decreasing of rubber particles size in TPVs lead to more effective stress localization, and then the elastic recovery is improved.[37] Therefore, this may also be the reason why PBS/EB-*g*-MAH showed better elastic recovery.

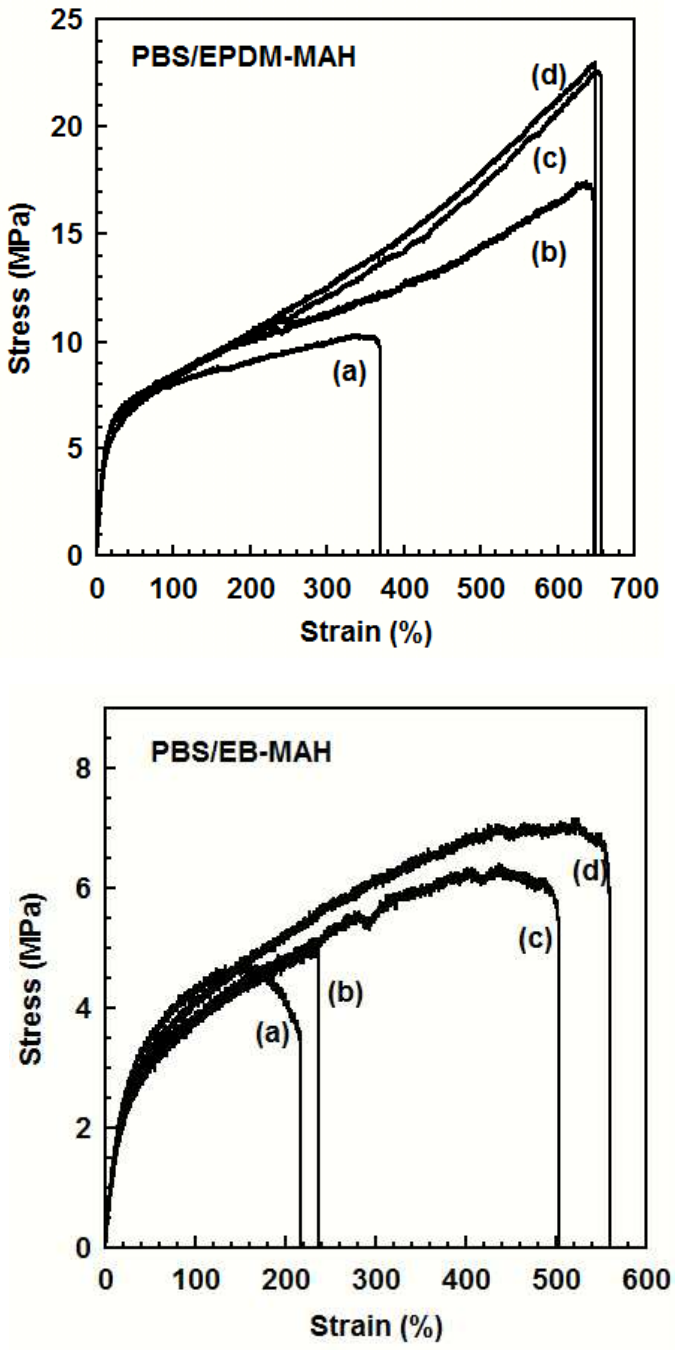

FIGURE 2.5 Stress-strain curves of PBS/EPDM-*g*-MAH and PBS/EB-*g*-MAH blends annealed at 170 ^{o}C for (a) 0, (b) 10, (c) 30 and (d) 60 min.

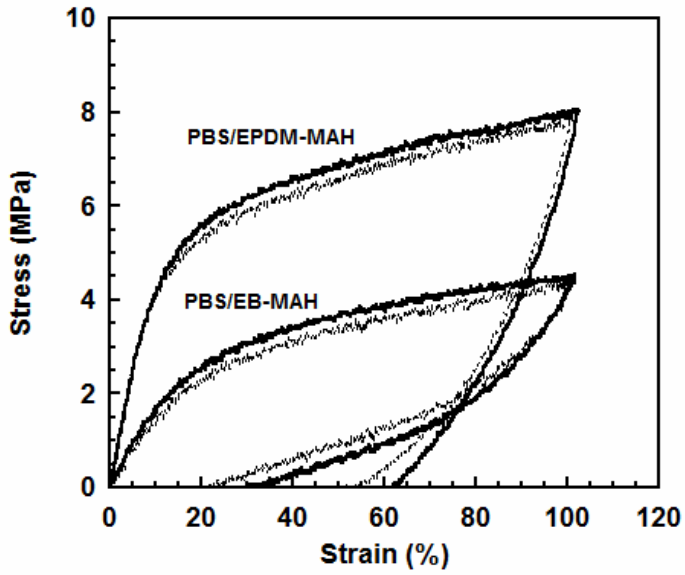

FIGURE 2.6 Strain recovery curves for PBS/EPDM-*g*-MAH and PBS/EB-*g*-MAH blends without annealing (bold line) and with annealing (thin line).

2.3.5 Annealing Effect on Interfacial Adhesion

In the SEM images of non-annealed PBS/EPDM-*g*-MAH and PBS/EB-*g*-MAH blends, the rubber particles were observed, and some of the particles were removed from PBS fracture surface as shown in Figure 2.2 (a) and (b). The annealed PBS/EPDM-*g*-MAH and PBS/EB-*g*-MAH blends showed smooth fracture surface as shown in Figure 2.7 (a) and (b), and the removing of rubber particles was not observed. The smooth fracture surface indicates that the fracture did not occur at the interface of matrix and dispersed phases by freeze-fracture in liquid nitrogen. Such a change in SEM fracture surface image by increasing of the interfacial adhesion has also been reported.[38] From the result, it was suggested that the annealing at 170 ^{o}C for 60 min improved interfacial adhesion between PBS and EPDM-*g*-MAH or EB-*g*-MAH rubber.

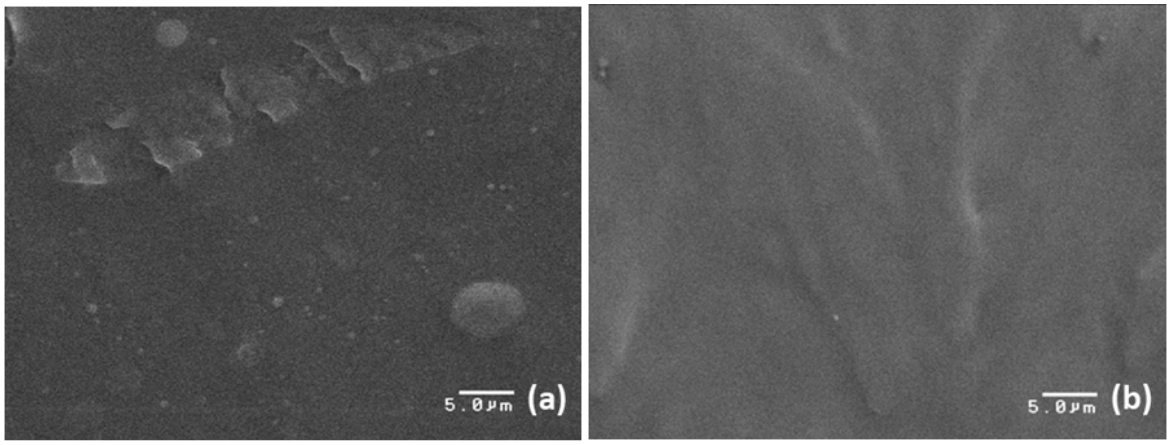

FIGURE 2.7 SEM pictures of fracture surface of (a) annealed PBS/EPDM-*g*-MAH and (b) annealed PBS/EB-*g*-MAH blends at 170 ^{o}C for 60 min.

To check the reaction by the annealing, the reacted component of PBS/EB-*g*-MAH and PBS/EPDM-*g*-MAH with annealing at 170 ^{o}C for 60 min was extracted by dissolving in chloroform for removing of unreacted PBS and rubbers phase. Although PBS, EPDM and EB can dissolve in chloroform, insoluble gel fractions of the annealed samples remained after extraction. These residual gel fractions were suggested to be the cross-linked samples, which were formed during both the mixing process and the annealing process. Deuri and Bhowmick also found a gel of raw EPDM rubber after extraction by the solvent, and this gel content increased with aging time without any compounding ingredients.[39] It is well known that the rubber without compounding ingredients also forms a cross-link by thermal aging.[39] Figure 2.8shows the DSC heating curves of PBS and annealed blend samples of PBS/EPDM-*g*-MAH and PBS/EB-*g*-MAH. DSC curves of EPDM and EB rubber showed a broad endothermic peak around 60 ^{o}C, which corresponded to the melting of crystal in rubbers[40,41] [Figure 2.8 (d)].The DSC heating curves of extracted component of annealed samples [Figure 2.8 (c)]

showed similar behavior with that of the blended samples with annealing [Figure 2.8 (b)], which showed both the crystal melting peaks of rubbers and PBS. However, the melting peak intensity of PBS was found to decrease, and it was due to a few amount of crystalline PBS. The result that the residual gel of annealed samples contained both rubber and PBS, indicates that the reaction occurred not only in the rubber phase but also at the interface between the PBS matrix phase and rubber dispersed phase.

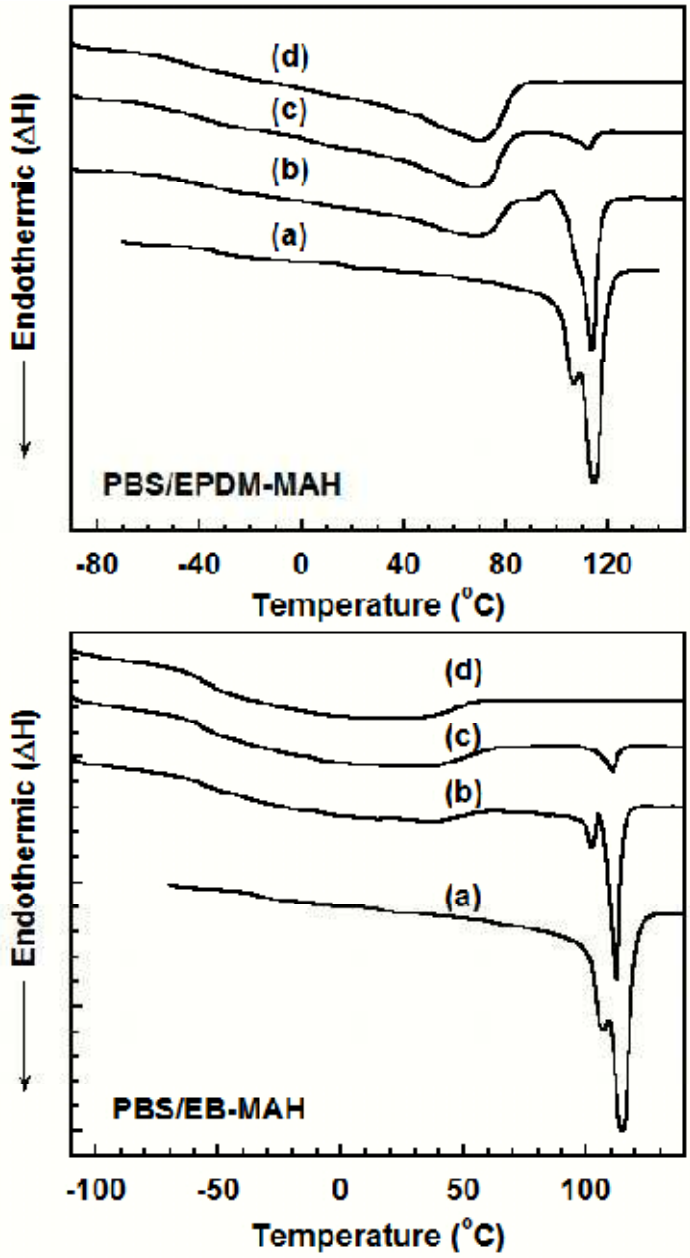

FIGURE 2.8 DSC heating curves of (a) neat PBS, (b) blend samples with annealing at 170 °C for 60 min, (c) solvent-extracted fractions of annealed samples and (d) neat rubbers.

Figure 2.9 shows FTIR spectra of the neat polymers, the blended samples with annealing at 170 ^{o}C for 60 min and solvent-extracted annealed samples by chloroform at 25 ^{o}C for 24 h. The absorption bands at 1720 cm^{-1} and 1163 cm^{-1} were assigned to the vibration of carbonyl (C=O) and ether groups (C-O-C) of PBS respectively.[42] In the EPDM-*g*-MAH and EB-*g*-MAH rubbers, the absorption band of C=O of MAH was located at 1709 cm^{-1}.[43] The spectra of annealed PBS/EPDM-*g*-MAH and PBS/EB-*g*-MAH showed the combined absorption bands of PBS and rubbers. Complication in the spectrum arose when the carbonyl band in the reactive groups and ether band in PBS overlapped. To overcome this complication, unreacted PBS in the blend was extracted by dissolving in chloroform. It was expected that if no reaction took place between PBS and the rubber, then PBS should be completely removed from the residual rubber, and the FT-IR spectrum of the solvent-extracted annealed fractions would have no contribution from PBS. However, in the extracted annealed fractions showed two weak absorption bands of C=O and C-O-C of PBS at 1720 cm^{-1} and 1163 cm^{-1} respectively [Figure 2.9 (c)]. These bands were found in the extracted annealed fractions of both blends. From these results it was suggested that PBS molecules were involved in the interfacial reaction, and the result agreed with that of DSC.

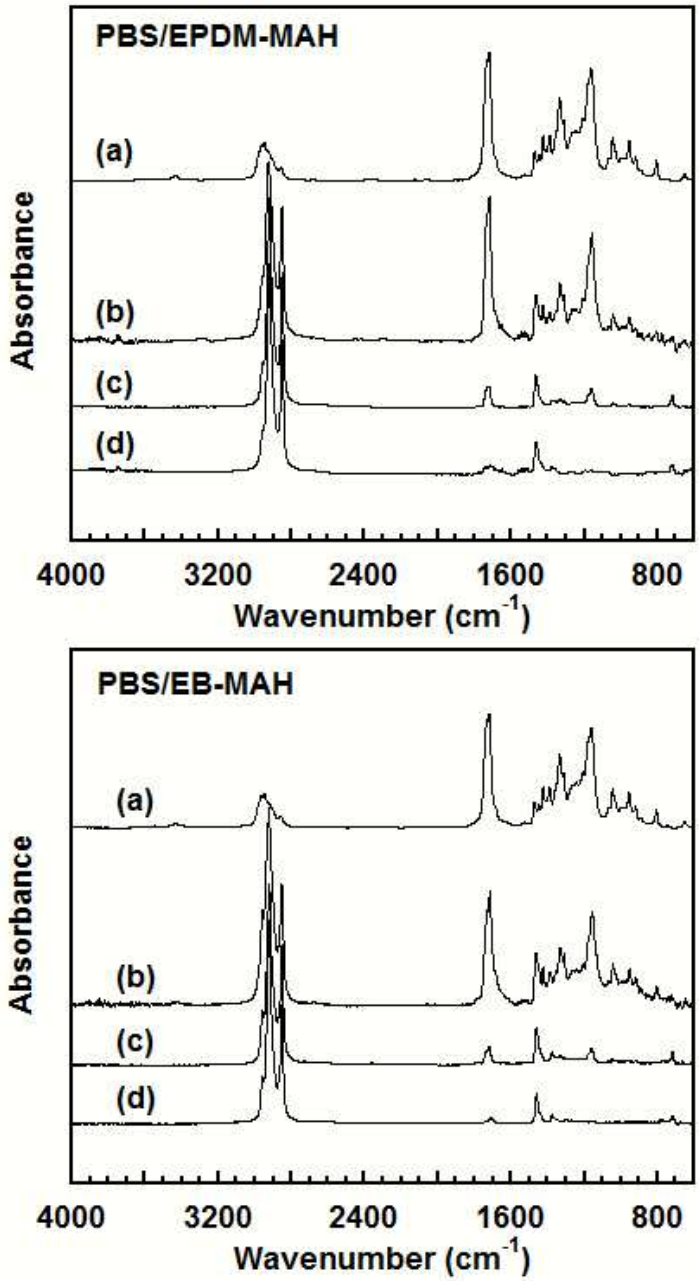

FIGURE 2.9 FTIR absorption spectra of (a) neat PBS, (b) blend samples with annealing at 170 ^{o}C for 60 min, (c) solvent-extracted fractions of annealed samples and (d) neat rubbers.

It is known that MAH can react with both hydroxyl group and carboxyl group under suitable condition[44] (the expected chemical reactions are shown in Scheme 2.4), but the reactivity of MAH is low.[14-16] Consequently, the annealing induced the additional reaction between terminal groups of PBS and MAH, and it led to the formation of Crosslinking structure at the interface. However, the annealing process may increase not only the interfacial reaction, but also the Crosslinking inside of the rubber phase.

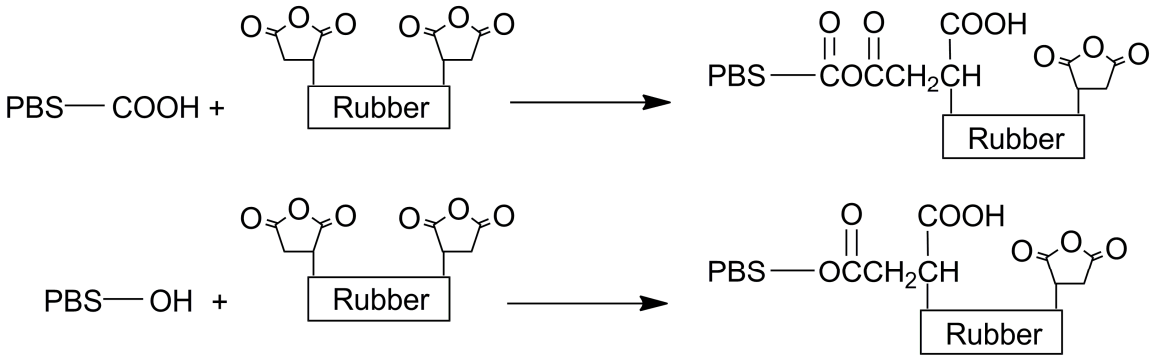

SCHEME 2.4 Expected reactions of PBS terminal groups and MAH group of rubber.

2.3.6 Influence of Annealing on Crosslinking

To check the Crosslinking in the rubber phase, the degree of Crosslinking was determined by dissolving the blends into chloroform at 25 ^{o}C for 24 h. Cross-linked components were not dissolved in this solvent. Annealing time dependence of the gel content of PBS/EPDM-*g*-MAH, EPDM-*g*-MAH, PBS/EB-*g*-MAH and EB-*g*-MAH are presented in Figure 10. PBS/EPDM-*g*-MAH blend and EPDM-*g*-MAH [Figure 2.10 (a)

and (b)] showed that the gel content after dissolving in chloroform increased with the annealing time. PBS/EB-*g*-MAH blend [Figure 2.10 (c)] showed a slightly increased gel content, while EB-*g*-MAH [Figure 2.10 (d)] showed almost no change with the annealing time. Formation of interfacial Crosslinking between the PBS matrix and the rubber dispersed phase during melt-mixing process was also suggested from the result, because both blended samples showed higher amount of gel contents than the rubbers alone even at the annealing for 0 min. It was suggested that the increased gel content by the annealing was due to the increase of both the Crosslinking of rubber and the interfacial reaction between PBS and the rubbers. EPDM without Crosslinking agent has low reactivity to form cross-link, but the reactivity increases by the increasing of aging temperature and time.[39] The higher gel content of annealed PBS/EPDM-*g*-MAH blend than annealed PBS/EB-*g*-MAH blend was attributed to the diene unit in EPDM. EB-*g*-MAH rubber was not cross-linked by the annealing at 170 ^{o}C for 60 min. The slightly increased gel content of annealed PBS/EB-*g*-MAH blend suggested the increased interfacial cross-link by the annealing. It was indicated that the increasing of both the Crosslinking of rubber and the interfacial cross-link by annealing were the reasons for the improvement of mechanical properties of PBS/MAH grafted rubber blends.

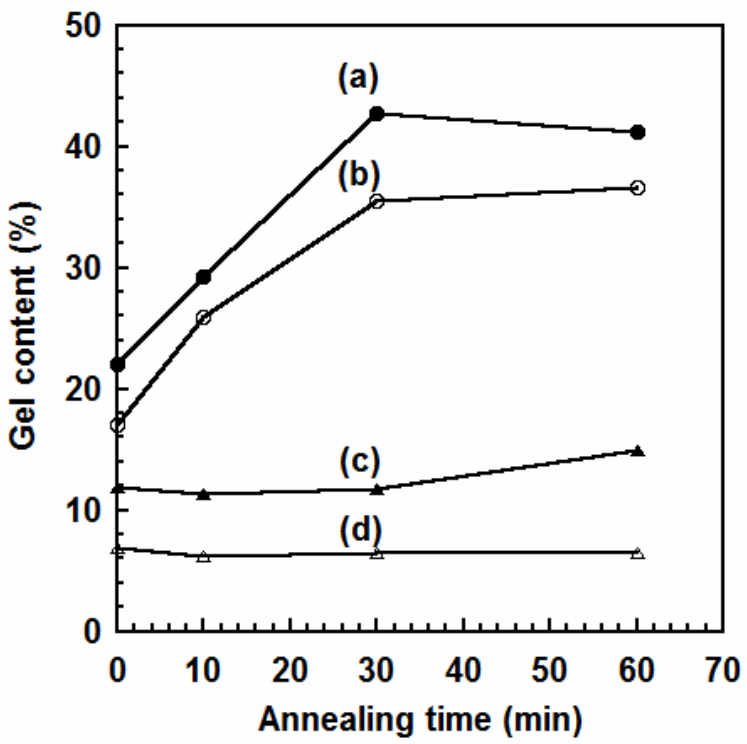

FIGURE 2.10 Variation of gel percentages with annealing time at 170 °C in (a) PBS/EPDM-*g*-MAH blend, (b) EPDM-*g*-MAH, (c) PBS/EB-*g*-MAH blend and (d) EB-*g*-MAH.

2.4 CONCLUSIONS

New TPEs of PBS/EPDM-*g*-MAH and PBS/EB-*g*-MAH with excellent tensile strength and strain recovery properties were successfully developed by the reactive blending and the annealing. Both blends showed the phase separated morphology, where the rubber particles were dispersed in the PBS matrix. The mechanical properties of them were improved by the annealing. The annealing process was found to have a two-fold effect: it improved the interfacial adhesion through the reaction between the

PBS terminal groups and the MAH group of the rubbers, and also promoted Crosslinking of EPDM rubber. The improved tensile strength of PBS/EPDM-*g*-MAH blend was due to the high Crosslinking of interfacial and rubber phase, while PBS/EB-*g*-MAH blend showed the better strain recovery because of the increased interfacial cross-link, the presence of small rubber particle dispersed in the PBS matrix and the better elasticity of EB rubber.

2.5 REFERENCES

1. Mishra, J. K.; Chang, Y. K.; Kim, D. K. *Mater. Lett*. **2007**, 61, 3551.
2. Tasdemir, M.; Topsakaloglu, M. *Int. J. Polym. Mater*. **2006**, 55: 1065.
3. Wang, R.; Wang, S. F.; Wan, C. Y.; Ma, P. *Polym. Eng. Sci*. **2009**, 49: DOI 10.1002/pen.21210.
4. Li, Y.; Kadowaki, Y.; Inoue, T.; Nakayama, K; Shimizu, H. *Macromolecules* **2006**, 39, 4195.
5. Jha, A.; Bhowmick, A. K. *J. Appl. Polym. Sci.* **2000***,* 78, 1001.
6. Jen, T.; Shui, L. *J. Appl. Polym. Sci.* **2009***,* 114, 2806.
7. Zhao, Y.; Yin, B.; Yang, M. B.; Feng, J.M. *Polym.-Plast. Technol. Eng*. **2007**, 46, 175.
8. Palmlof, M.; Hjertberg, T. *J. Appl. Polym. Sci*. **1999**, 72, 521.
9. Soares, B. G.; Oliveira, M. D.; Meireles, D.; Sirqueira, A.S.; Mauler, R.S. *J. Appl. Polym. Sci.* **2008**, 110, 3566.

10. Shi, Q.; Stagnaro, P.; Cai, C. L.; Yin, J. H.; Costa, G.; Turturo, A. *J.Appl. Polym. Sci.* **2008**, 110, 3963.
11. Nakason, C.; Saiwaree, S.; Tatun, S.; Kaesaman, A. *Polym. Test.* **2006**, 25, 656.
12. Saelao, J.; Phinyocheep, P. *J.Appl. Polym. Sci.* **2005**, 95, 28.
13. Ho, C. H.; Wang, C. H.; Lin, C.I.; Lee, Y.D. *Polymer* **2008**, 49, 3902.
14. Rao, H.; Zhang, Z.*Polym. Adv. Technol.* **2008**, 19, 770.
15. Bevington, J. C.; Johnson, M. *Eur. Polym. J.* **1966**, 2, 185.
16. Li, Y.; Xie, X.M.; Guo, B.H. *Polymer* **2001**, 42, 3419.
17. Grigiryeva, O.P.; Kocsis, J.K. *Eur. Polym. J.* **2000**, 36, 1419.
18. Aravind, I.; Albert, P.; Ranganathaiah, C.; Kurian, J. V.; Thomas, S. *Polymer* **2004**, 45, 4925.
19. Mehrabzadeh, M.; Nia, H. K. *J. Appl. Polym. Sci.* **1999**, 72, 1257.
20. Carone Jr. E.; Kopcak, U.; Concalves, M. C.; Nunes, S. P. *Polymer* **2000**, 41, 5929.
21. Nakason, C.; Kaesman, A.; Samoh, S.; Homsin, S.; Kiatkamjornwong, S.*Polym. Test.* **2001**, 21, 449.
22. Kim, S. J.; Shin, B. S.; Hong, J. L.; Cho, W. J.; Ha, C. S., *Polymer* **2001**, 42, 4073.
23. Mishra, J. K.; Ryou, J. H.; Kim, G. H.; Hwang, K. J.; Ha, C. S. *Mater. Lett.* **2004**, 58, 3477.
24. Sen, A.; Bhattacharya, M. *Polymer* **2002**, 41, 9177.
25. Li, T. Q.; Ng, C. N.; Li, R. K. Y. *J. Appl. Polym. Sci.* **2001**, 81, 1420.

26. Nakason, C.; Kaesman, A.; Homsin, S.; Kiatkamjornwong, S. *J. Appl. Polym. Sci*. **2001**, 81, 2803.
27. Li, H. M.; Chen, H. B.; Shen, Z. G.; Lin, S. *Polymer* **2002**, 43, 5455.
28. Li, C.; Zhang, Y.; Zhang, Y.*Polym. Test*. **2003**, 22, 191.
29. Shujun, W.; Jiugao, Y.; Jinglin, Y. *Polym. Degrad. Stab.* **2005**, 87, 395.
30. Phan, T. T. M.; De Nicola, A. J.; Schadler, L. *J. Appl. Poly. Sci.* **1998**, 68, 1451.
31. Kim, J. H.; Lee, J.H. *Polymer* **2002**, 34, 203.
32. Wanamaker, C.L.; Bluemle, M.J.; Pitet, L.M.; O'Leary, L.E.; Tolman, W.B.; Hillmyer, M.A. *Biomacromolecules*. **2009**, 10, 2904.
33. Mohanty, A.K.; Misra, M.; Hinrichsen, G. *Macromol. Mater. Eng*. **2000**, 276, 1.
34. Willke, T.; Vorlop, K.D., *Appl. MicrobiolBiotechnol.* **2004**, 66, 131.
35. Lui, Y.; Ranucci, E.; Lindblad, M.S.; Albertsson, A.C. *J. Bioactive. Compat. Polym*. **2002**, 17, 209.
36. Kikuchi. Y.; Fukui, T.; Okada, T.; Inoue, T. *J. Appl. Polym. Sci.* **1991**, 49, 1029.
37. Roy, M. A. I.; Martin, V. D.; Anne, B. S.; Johannes, G.P. *Soft Matter.* **2010**, 6, 1758.
38. Liu, H.; Guo, L.; Guo, X.; Zhang, J. *Polymer* **2012**, 53, 272.
39. Deuri, A.S.; Bhowmick, A.K. *J. Appl. Poly. Sci.* **1987***,* 34, 2205.
40. Sichina, W. J., Thermal Analysis Application Note. (accessed February 14, 2011).http://las.perkinelmer.com/Content/applicationnotes/app_thermalepdmelastomersusingdsc.pdf
41. Eynde, S.V.; Mathot, V.; Koch, M.H.J.; Reynaers, H. *Polymer* **2005**, 41, 3437.
42. Han, Y. K.; Kim, S. R.; Kim, J. *Macromol. Res.* **2002**, 10, 108.

43. Barra, G. M. O.; Crespo, J. S.; Bertolino, J. R.; Soldi, V.; Pires, A. T. N. *J. Braz. Chem. Soc.* **1999**, 10, 31.

44. Kim, S. J.; Shin, B. S.; Hong, J. L.; Chob, W. J.; Ha, C. S. *Polymer* **2001**, 42, 4073.

CHAPTER 3

Thermoplastic Elastomer by Reactive Blending of Poly(butylene succinate) with Acrylic Rubber

3.1 INTRODUCTION

Poly(butylene succinate) (PBS), is a biodegradable plastic with excellent processing ability and fast crystallization rate.[1] The chemical structure of PBS is presented in scheme 2.1 (Chapter 2). PBS is derived from butanediol and succinic acid. Though these two kinds of monomers used to polymerize the commercial PBS is currently made from petroleum resources, innovative technology to produce bio-based succinic acid and butanediol has been developed and then bio-based PBS will be commercialized in the near future.[2-4] The mechanical properties of PBS are similar to polyethylene and polypropylene[5]. PBS has excellent processability and can be processed on polyolefin processing machines.[6] Because of the advantages described above, PBS is a potential material for development of a new thermoplastic elastomer (TPE) by a biodegradable plastic.

Acrylic rubber (ACM) is a vulcanizable rubber. It has good resistance to heat and oil, and it has excellent processability because of its low viscosity.[7] The chemical

structure of ACM is shown in scheme 3.1. ACM was used for this investigation by the reason of excellent elastic properties and low viscosity. We expected that the less viscosity difference between PBS and ACM induces the fine morphology, because the size of dispersed particles in a blend depends on the viscosity ratio of component polymers.

Literatures have shown many systems of polymer blends with elastomers.[8-14] For the improvement of mechanical properties in the polymer blend, dicumyl peroxide (DCP) of which the chemical structure is shown in Scheme 3.2 was employed to enhance interfacial reaction between matrix and dispersion phases.[12-14] DCP is an initiator for the polymerization and vulcanization, and it is used to initiate free radical and to induce reactions in the blend. Poly[methylene (phenyleneisocyanate)] (PMPI) was used as coupling agent for the component polymers of the blend to improve blend morphology and interfacial adhesion between matrix and dispersion phases by improving the compatibility.[15-16] The chemical structure of PMPI is shown in Scheme 3.3. The isocyanate group of PMPI can react with terminal groups of thermoplastics such as hydroxyl group and carboxyl group during melt mixing process. In some polymer blends such as polyamide/poly(phenylene sulfide) and poly(ethylene terephthalate)/polystyrene/poly(stylene-*co*-maleic anhydride) blends, compatibility, morphology and mechanical properties were improved by addition of PMPI.[15-16] Various types of thermoplastics were blended with ACM, such as polybutylene terephthalate,[8] polyvinylidene difluoride,[9] polyamide[10] and polyethylene terephthalate.[11] It was considered that DCP and PMPI were also effective for PBS blend, however, the effect of them on PBS/rubber blend has not been reported as for my knowledge.

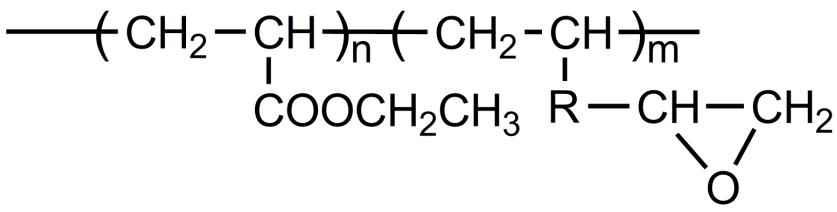

SCHEME 3.1 Chemical structure of ACM

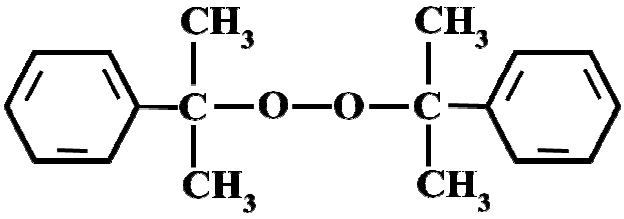

SCHEME 3.2 Chemical structure of DCP.

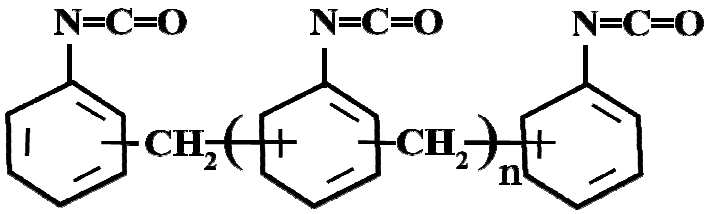

SCHEME 3.3 Chemical structure of PMPI.

3.1.1 Objective of this Chapter

In this chapter, a biodegradable TPE was developed by PBS/ACM blend by using two kinds of chemicals, DCP and PMPI. Their morphology, rheological, thermal

properties and mechanical properties were investigated. The relationship between the reaction in the blend and properties was also considered.

3.2 EXPERIMENTAL

3.2.1 Materials

Detail about PBS was given in Chapter 2. ACM with epoxy cure site (NIPOL AR51) was supplied by ZEON Co., Ltd. PMPI was kindly supplied by Mitsui chemicals polyurethanes, Inc. DCP was purchased from Sigma-Aldrich, Inc.

3.2.2 Measurements

3.2.2.1 Samples Preparation

The PBS/ACM blend (40/60, wt%/wt%) was prepared by using two different methods. First, PBS was melt-mixed with ACM at 160 ^{o}C. 2 phr of DCP was added during the mixing time at 2 min, and then the blend was continued to mix for 10 min. Secondly, ACM was pre-mixed with 1.0 phr of PMPI and 0.5 phr of DCP for grafting PMPI onto ACM at 100 ^{o}C for 5 min. Then PMPI grafted with ACM rubber (ACM-PMPI) was mixed with PBS at 160 ^{o}C for 10 min without addition of peroxide. The formulations are shown in Table 3.1.

Table 3.1 Mixing formulation of PBS and ACM blends with DCP or PMPI

Samples	PBS (%)	ACM (%)	DCP (phr)	PMPI (phr)
PBS/ACM	40	60	-	-
PBS/ACM/DCP	40	60	2	-
PBS/ACM-*g*-PMPI	40	60	0.5	1

3.2.2.2 Phase Determination

PBS/ACM/DCP, PBS/ACM-*g*-PMPI and PBS/ACM blends were dissolved in chloroform by the concentration of 0.01 g/ml. The mixture solution was left to stand for at least 24 h, and then the component of matrix and dispersed phase was checked from the residual component.

3.2.2.3 Differencial Scanning Calorimetry (DSC)

The measurement was similar to that given in Chapter 2. Glass transition temperature (T_g), melting temperature (T_m) and crystallization temperature (T_c) were measured. Crystallinity (X_c) was estimated by the following equation:

$$X_c(\%) = \frac{\Delta H_m}{\Delta H_m^0} \times 100 \tag{3.1}$$

where ΔH_m is the heat of fusion of the sample, and ΔH_m^o is that of perfect crystal (200 J/g for PBS).[17]

3.2.2.4 Tensile Properties Measurements

As given in Chapter 2.

3.2.2.5 Scanning Electron Microscopy (SEM)

SEM (SM-200, Topcon Corp.) was used to investigate the morphology of the blends. The samples were broken in liquid nitrogen, and then the rubber particles were extracted from fracture surface by the immersion into tetrahydrofuran (THF) at room temperature for 24 h. The fracture surface of samples were coated with thin-layer of gold, and observed with an acceleration voltage of 10 kV.

3.2.2.6 Rheological Measurement

The complex dynamic viscosity (η^*) was measured by a rheometer (Dynamic Analyzer RDA II, Rheometric Scientific Corp.). The samples were prepared by the compression molding to a disc with thickness of 1 mm and diameter of 25 mm. The measurement was carried out at frequencies in the range from 0.1 to 1000 rad/s at strain rate of 10% and the constant temperature.

3.3 RESULTS AND DISCUSSION

3.3.1 Compatibility and Phase Determination

Figure 3.1 shows the visual image of the PBS/ACM/DCP, PBS/ACM-*g*-PMPI and PBS/ACM. It was clearly observed that PBS/ACM/DCP and PBS/ACM-*g*-PMPI

blends were homogeneous, while PBS/ACM was inhomogeneous. The image indicated that DCP and PMPI improved the compatibility between PBS and ACM.

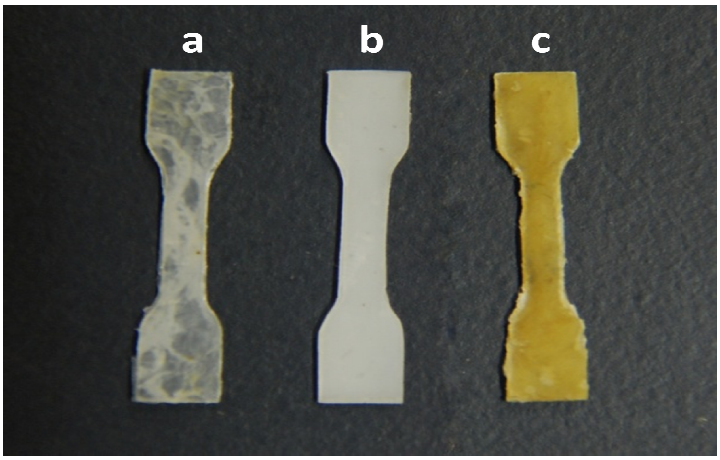

FIGURE 3.1 Image of the samples of (a) PBS/ACM, (b) PBS/ACM/DCP and (d) PBS/ACM-*g*-PMPI blends.

Phase determination was carried out to evaluate the polymer constituting the matrix phase. As shown in Figure 3.2, the PBS/ACM-*g*-PMPI and PBS/ACM/DCP blends were dissolved in chloroform, and they exhibited apparent residual particles. On the contrary, in the case of PBS/ACM blend, the sample was completely dissolved into the solvent. Pure PBS and ACM were completely dissolved by this solvent. Therefore, the residual particles of the blend in the solution after dissolution were supposed to be crosslinked rubber particles and copolymer consisting of PBS and ACM. From these results, it was indicated that the ACM particles were dispersed in PBS matrix. Both Crosslinking of rubber phase and Crosslinking between PBS and ACM interface might be generated by addition of DCP and PMPI chemicals.

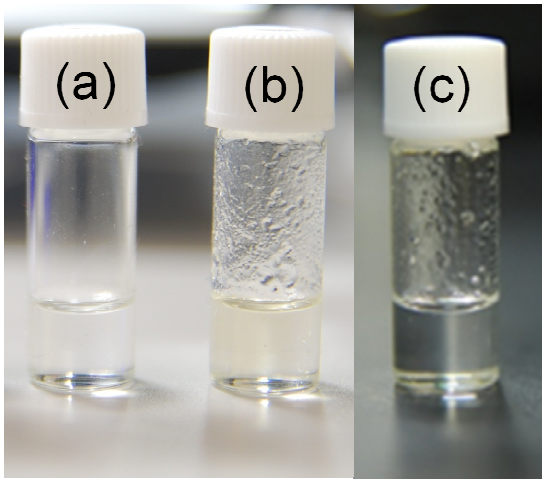

FIGURE 3.2 Phase determination of (a) PBS/ACM (b) PBS/ACM-*g*-PMPI (c) PBS/ACM/DCP blends.

3.3.2 Tensile Properties

Figure 3.3 shows the stress-strain curves of PBS/ACM/DCP, PBS/ACM-*g*-PMPI and PBS/ACM. In the PBS/ACM/DCP blend, maximum tensile strength and elongation at break were improved, while PBS/ACM-*g*-PMPI blend was not improved. However, the modulus decreased in the blend with addition of PMPI. Table 3.2 shows tensile properties of PBS, PBS/ACM, PBS/ACM/DCP and PBS/ACM-*g*-PMPI blends. Maximum tensile strength, modulus and elongation at break of PBS/ACM blend showed lower than those of PBS. It was understood to be due to the increasing of soft rubber component, ACM rubber. However, elongation at breaks of the blended samples were lower than that of PBS due to low interfacial adhesion between PBS and ACM phases. In the PBS/ACM/DCP blend, the modulus of the blend was 33 MPa, which was the same value with PBS/ACM. In the PBS/ACM-*g*-PMPI blend, the modulus reduced

to 4 MPa. However, in the PBS/ACM/DCP blend, the maximum tensile strength and elongation at break increased to 11.9 MPa and 177% respectively. In PBS/ACM-*g*-PMPI blend, maximum tensile strength and elongation at break decreased to 2.7 MPa and 75% respectively. It was indicated that maximum tensile strength and elongation at break were enhanced with addition of DCP due to the increasing of interfacial reaction.[18] The improvement of mechanical properties and the reaction mechanisms in polyester blends by addition of PMPI and DCP have also been reported.[13,19] Therefore, the tensile properties improvement of PBS/ACM/DCP blend was suggested to the increasing of interfacial reaction between PBS and ACM by DCP.

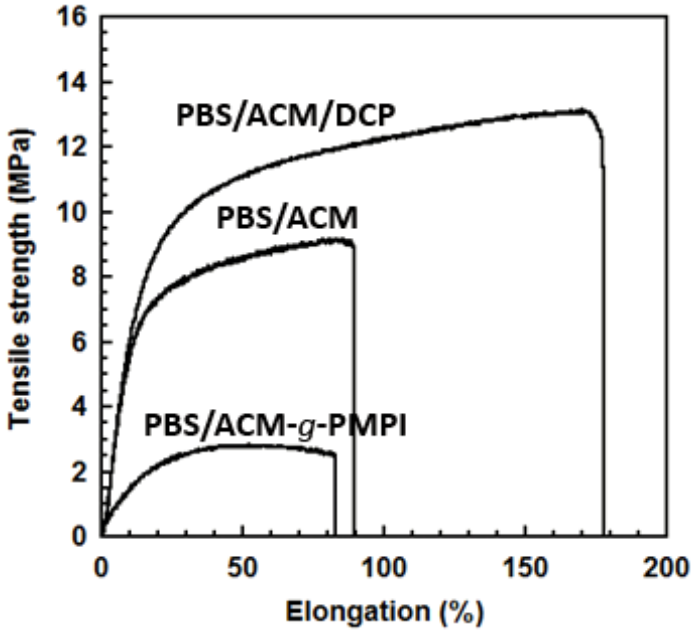

FIGURE 3.3 Stress-strain curves of PBS/ACM/DCP, PBS/ACM-*g*-PMPI and PBS/ACM.

Table 3.2 Tensile properties of PBS, PBS/ACM, PBS/ACM/DCP and PBS/ACM-*g*-PMPI blends.

Samples	Maximum tensile strength (MPa)	Modulus (MPa)	Elongation at break (%)
PBS	41.6	303	337
PBS/ACM	8.9	33	89
PBS/ACM/ DCP	11.9	33	177
PBS/ACM-*g*-PMPI	2.7	4	75

Figure 3.4 presents the strain recovery behavior of PBS/ACM/DCP, PBS/ACM-*g*-PMPI blends and the commercialized TPV, polypropylene (PP)/ethylene-propylene-diene terpolymer (EPDM) blend. PBS/ACM/DCP and PBS/ACM-*g*-PMPI blends showed the strain recovery behaviors similar to the commercialized PP/EPDM. It was suggested that the Crosslinking of ACM phase and the strong interfacial adhesion by the interfacial reaction provided this strain recovery.

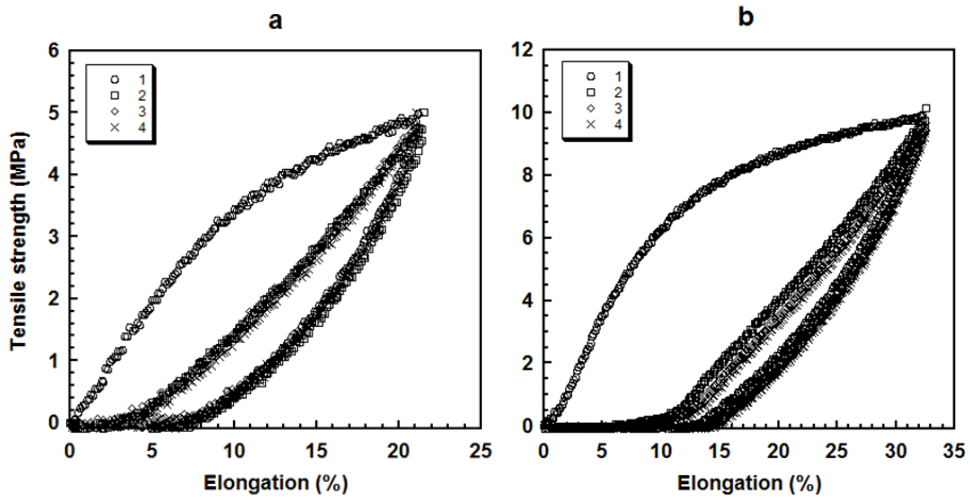

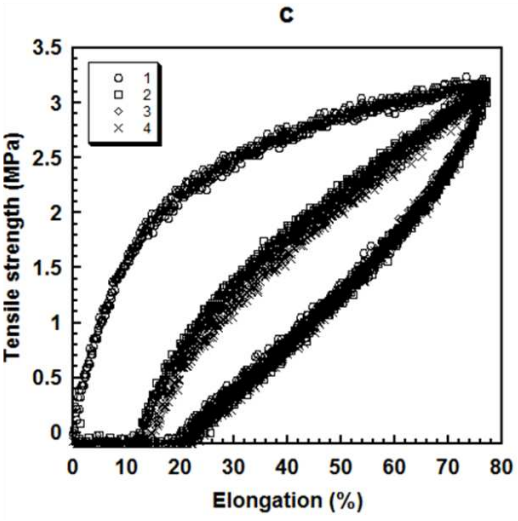

FIGURE 3.4 Strain recovery of (a) PBS/ACM-*g*-PMPI (b) PBS/ACM/DCP (c) PP/EPDM.

3.3.3 Thermal Analysis

Figure 3.5 shows DSC curves of PBS, PBS/ACM, PBS/ACM/DCP and PBS/ACM-*g*-PMPI blends. PBS showed multiple melting peaks in the DSC heating scan [Figure 3.5 (a)] as reported by many researchers.[20-23] Though PBS presents two types of crystals, α and β,[24-26] they do not contribute to the multiple melting peaks. Because β crystal is formed at low temperature, then it changes to α crystal at higher temperature. Therefore, crystal melting in this DSC scan is only α crystal. In PBS/ACM blend, the T_g showed only one T_g in the heating scan [Figure 3.5 (a)] because T_g of PBS and ACM appeared at nearly same temperature. Then, both T_g were combined to appear in one T_g. In cooling scan [Figure 3.5 (b)], crystallization peak of all blends appeared at almost the same temperature of T_c. Table 3.3 presents thermal properties and crystallinity of PBS, ACM, PBS/ACM, PBS/ACM/DCP and PBS/ACM-*g*-PMPI

blends. PBS/ACM-*g*-PMPI blend showed the decreasing of crystallinity compared to PBS/ACM, while PBS/ACM/DCP blend was not changed. The crystallinities of PBS in all the blends hardly changed from neat PBS, and it was indicated that the decreasing of modulus in PBA/ACM-g-PMPI was not due to the low crystallinity. Therefore, the morphology was observed by SEM.

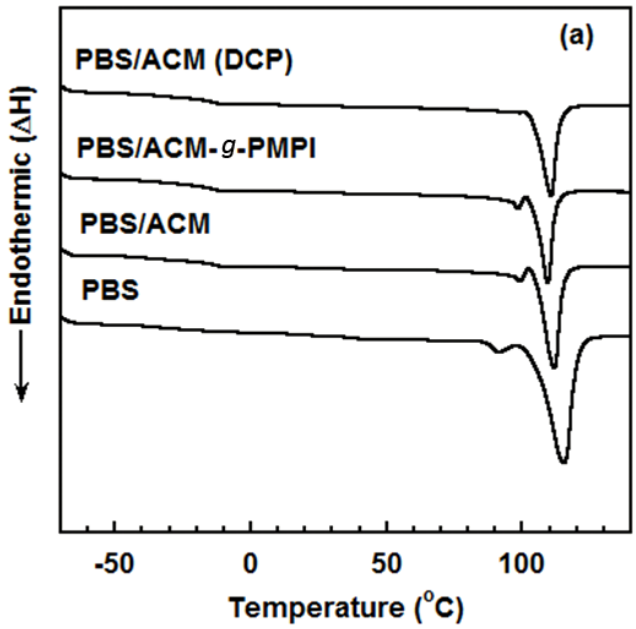

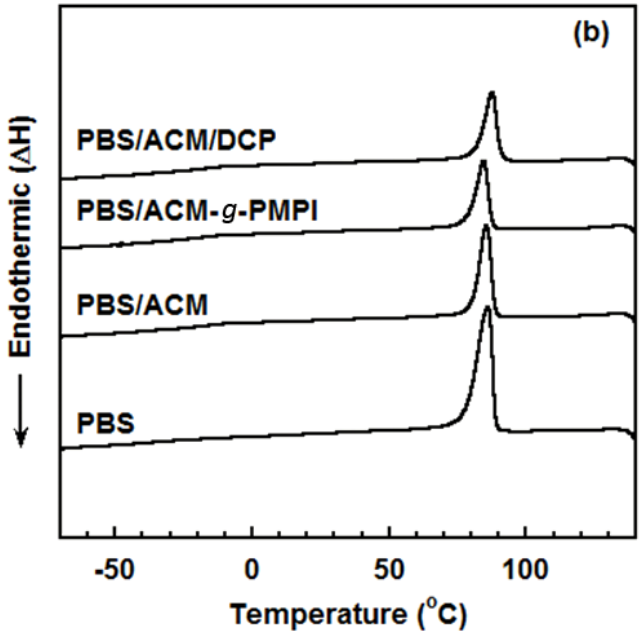

FIGURE 3.5 DSC heating scan (a) and cooling scan (b) of PBS and ACM blend at a rate of 10°C/min.

Table 3.3 Thermal properties and crystallinity of PBS, ACM and PBS/ACM blend

Sample	T_g (°C)	T_m (°C)	T_c (°C)	Crystallinity (%)
ACM	-13.6	-	-	-
PBS	-32.9	115.4	85.8	35
PBS/ACM	-17.7	112.3	84.8	34
PBS/ACM/DCP	-16.9	110.8	86.5	34
PBS/ACM-*g*-PMPI	-17.5	109.7	87.6	31

3.3.4 Morphology

Figure 3.6 shows SEM micrographs of fractured surface of PBS/ACM/DCP and PBS/ACM-*g*-PMPI blends. The rubber phase was extracted by immersion into tetrahydrofuran for 24h. The holes in the images were due to uncrosslinked rubber phase that has been extracted by solvent. In PBS/ACM/DCP blend, ACM rubber particles were suggested to disperse in PBS matrix because holes formed by extraction of rubber phase were uniformly observed. The comparison between figures [Figure 3.6 (a) and (b)] presents that PBS/ACM/DCP blend shows smaller ACM rubber particles and uniform dispersion in PBS matrix than PBS/ACM-*g*-PMPI blend. It was considered that the reduction of domain size by addition of DCP was due to the reduction of interfacial tension through reaction at the interface by DCP during melt-mixing process, and it was in agreement with the results of Wang et al.[27] In contrast with it, in PBS/ACM-*g*-PMPI blend, bigger size of rubber particles and nonuniform dispersion were observed. From the result, it was suggested that the improvement of strain at break in PBS/ACM/DCP originated in the finer morphology. Moreover, it was also suggested that the compatibility of PBS and ACM-*g*-PMPI was less than that of PBS and ACM with DCP.

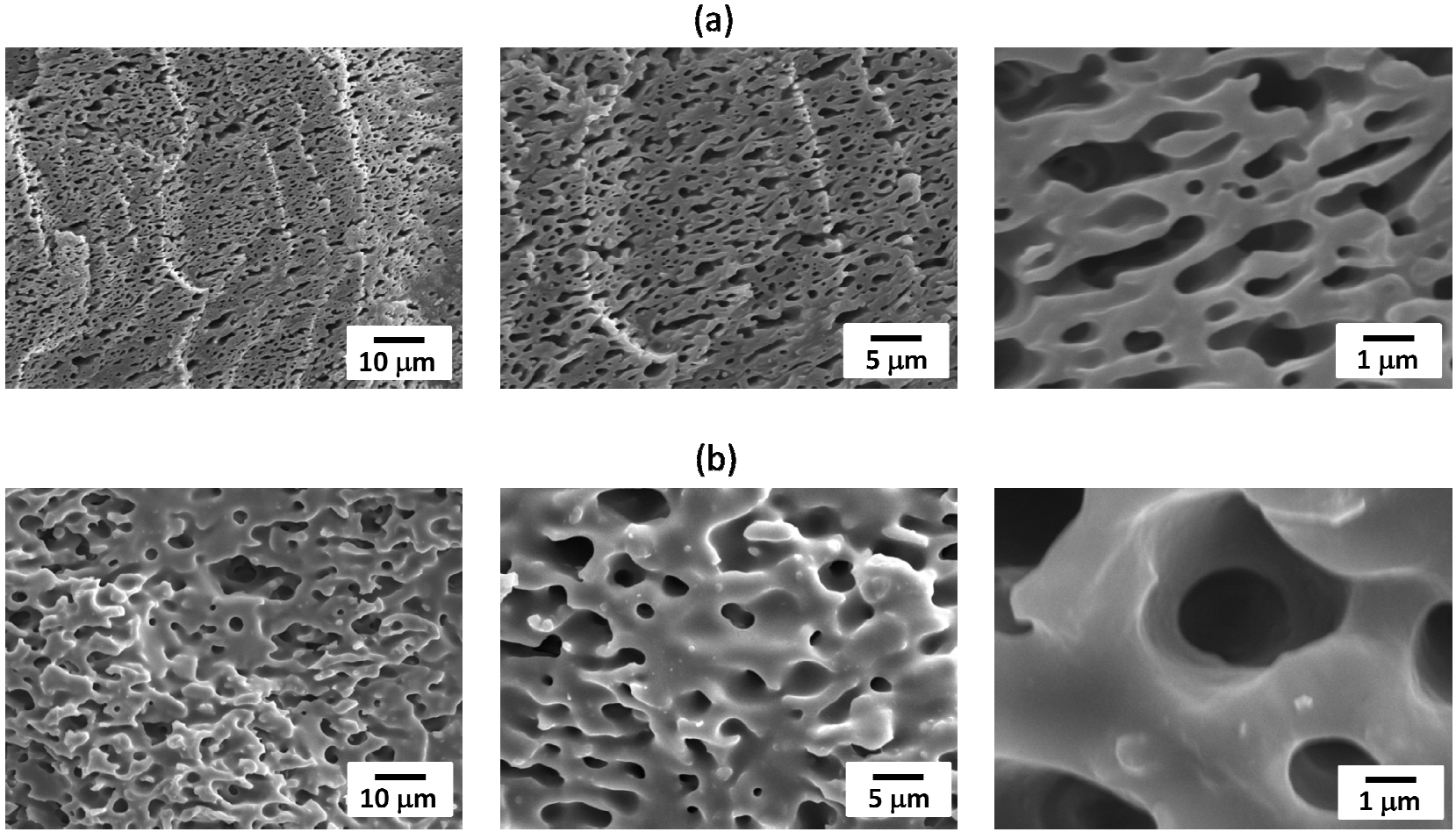

FIGURE 3.6 SEM micrographs of fractured surface of (a) PBS/ACM/DCP blend and (b) PBS/ACM-*g*-PMPI blend.

3.3.5 Rheological Analysis

The rheological behavior of PBS, ACM and PBS/ACM blends were measured at 150 ^{o}C, and the results are shown in Figure 3.7. The complex viscosity of PBS/ACM/DCP presented between pure PBS and ACM, while complex viscosity of PBS/ACM-*g*-PMPI blend showed almost similar trend to that of ACM. In PBS/ACM-*g*-PMPI blend, the complex viscosity was higher than PBS/ACM/DCP blend. When PMPI was added to PBS during melt-mixing process, obtained PBS/PMPI was not reprocessable. This fact indicated that the highly crosslinked structure was formed in PBS by addition of PMPI, because PMPI have more than two isocyanate groups in a molecule. In PBS/ACM-*g*-PMPI, the network structure must be also formed and then the blend showed higher viscosity. Figure 3.8 shows frequency dependence of complex viscosity of ACM, PBS, ACM-*g*-PMPI and PBS/ACM-*g*-PMPI blends. The complex viscosity at low frequencies of ACM rubber increased by addition of PMPI (1 phr) due to the increasing of crosslink. This indicated that PMPI increased crosslink reactions in both PBS and ACM which induced the increasing of complex viscosity. Figure 3.9 represents the frequency dependence of complex viscosity of ACM, PBS, ACM/DCP, PBS/DCP and PBS/ACM/DCP blends. The complex viscosity at low frequencies of PBS increased after addition of 2.0 phr of DCP. It was suggested that the DCP generated free radicals and induced grafting or Crosslinking reactions to form network structure in PBS. Wang et al. and Kim et al also reported similar results.[14,18] On the other hand, the complex viscosity at low frequencies of ACM rubber decreased after addition of DCP, which indicated to chain scission of ACM. All these indicated that PMPI reacted with both PBS and ACM, while DCP generated free radicals in both PBS

and ACM to induce a reaction. It was considered the reaction between PBS and ACM was also induced by addition of DCP and PMPI, which improved the compatibility of the blends. The expected reactions of PBS/ACM-*g*-PMPI and PBS/ACM/DCP blends are presented in Scheme 3.4 and 3.5 respectively.

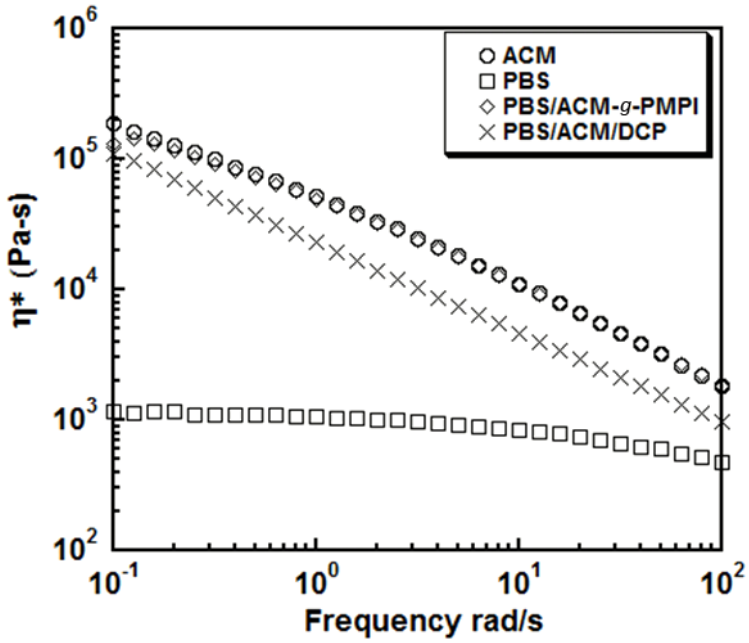

FIGURE 3.7 Frequency dependence of complex viscosity of ACM, PBS, PBS/ACM-*g*-PMPI and PBS/ACM with DCP.

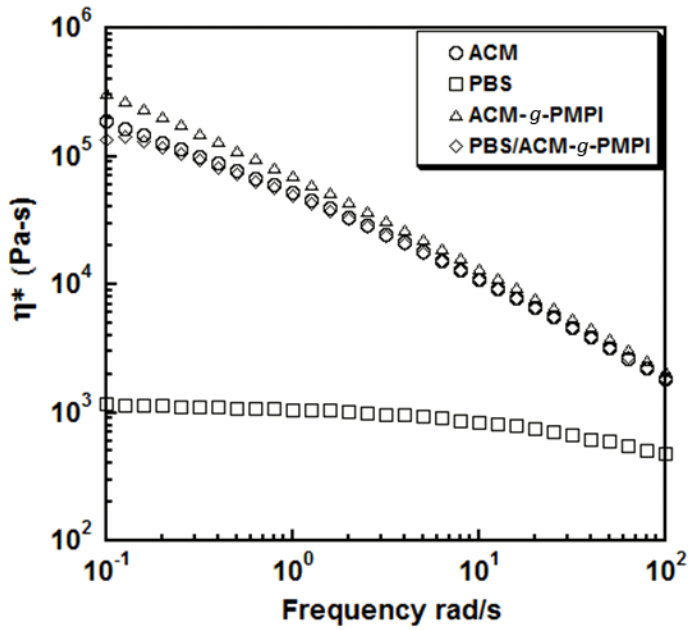

FIGURE 3.8 Frequency dependence of complex viscosity of ACM, PBS, ACM/PMPI and PBS/ACM-*g*-PMPI.

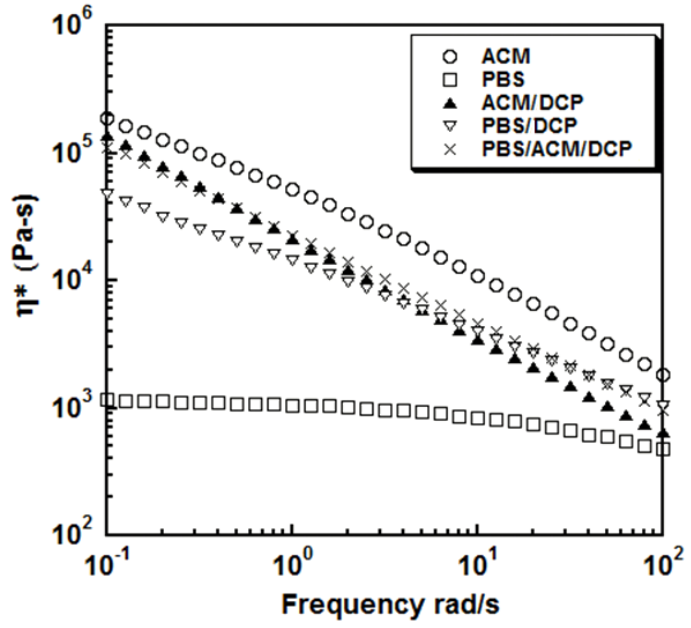

FIGURE 3.9 Frequency dependence of complex viscosity of ACM, PBS, ACM/DCP, PBS/DCP and PBS/ACM/DCP.

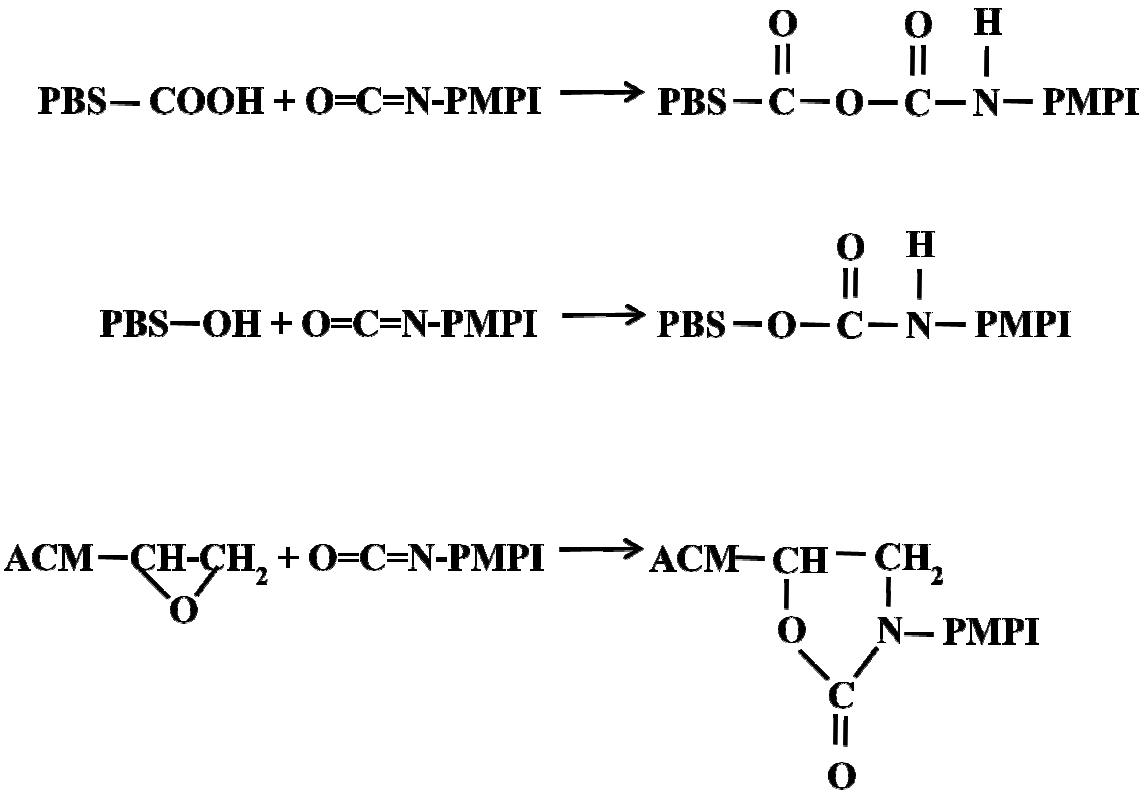

SCHEME 3.4 Expected reaction mechanism of PMPI with PBS or ACM.

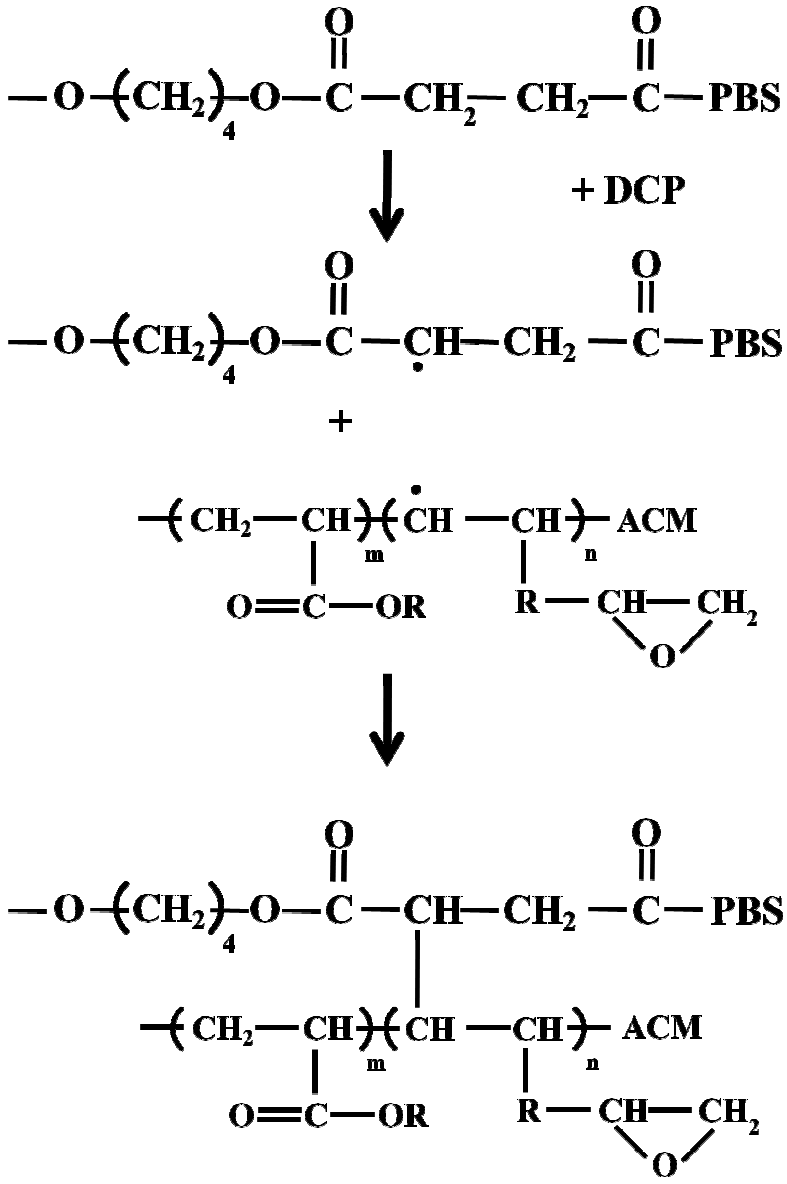

SCHEME 3.5 Expected reaction mechanism of PBS/ACM/DCP.

3.4 CONCLUSIONS

PBS/ACM blend was produced by melt mixing method with DCP or PMPI at high temperature. From the solubility test and SEM fracture surface images, it was confirmed that PBS and ACM are immiscible, and the ACM rubber particles are dispersed in PBS matrix. The increasing of interfacial adhesion by DCP markedly improved the elongation at break and maximum tensile strength. However, DCP induced the reaction not only at the interface but also inside of the PBS phase, and these reaction increased yield strength and tensile strength in the blend. In PBS/ACM-*g*-PMPI blend, bigger size of rubber particles and its nonuniform dispersion were observed. This reaction proceeded during grafting PMPI onto ACM process. It induced crosslink network structure in ACM, and increased viscosity difference between PBS and ACM. However, the blending with both chemicals, DCP and PMPI, did not contribute the thermal properties of the blend. From the comparison of PBS/ACM/DCP with PBS/ACM-*g*-PMPI blends, it was indicated that DCP was more efficient in compatibilizing the PBS/ACM blend. It related with smaller particle size, good dispersion, higher elongation at break, better tensile strength, and strain recovery behaved like rubber. These were due to the increase of interfacial reaction, which improved compatibility and properties of the blend.

3.5 REFERENCES

1. Papageorgiou, G.Z.; Dachilias, D.S.; Bikiaris, D.N. *Macromol. Chem. Phys.* **2007**, 208, 1250.
2. Lee, S.Y.; Hong, S.H.; Lee, S.H.; Park, S.J. *Macromol. Biosci.* **1988**, 4, 157.
3. Willke, T.;Vorlop, K.D. *Appl. Microbiol. Biotechnol.* **2004**, 66, 131.
4. Liu, Y.; Ranucci, E.; Lindblad, M.S. Albertsson, A.C. *J. Bioactive. Compat. Polym.* **2002**, 17, 209.
5. Mohanty, A.K.; Misra, M.; Hinrichsen, G. *Macromol. Mater. Eng.* **2000**, 276, 1.
6. Fujimaki, T. *Polym. Degrad. Stab.* **1998**, 59, 209.
7. Stammer, P.H. *Prog. Rubber Plast. Technol.* **1987**, 3, 1.
8. Jha, A.; Bhowmick, A.K. *J. Polym. Sci.* **2000**, 78, 1001.
9. Li,Y.; Oono, Y.; Kadowaki, Y.; Inoue, T.; Nakayama, K.; Shimizu, H. *Macromolecules* **2006,** *39,* 4195.
10. Shiva, K.E.; Yadaw, S.B.; Pandey, K.N.; Das, C.K. *Appl. Polym. Sci.* **2006**, 100, 3904.
11. AbhijitJha, A.; Bhowmick, A.K. *Polymer* **1997**, 38, 4337.
12. Tasdemir, M.; Topsakaloglu, M. *Polym. Mater.* **2006**, 55, 1065.
13. Mishra, J.K.; Chang, Y.K.; Kim, D.K. *Mater. Lett.* **2007**, 61, 3551.
14. Wang, R.; Wang, S.F.; Chaoying Wan, C.Y. *Polym. Eng. Sci.* 2009, DOI 10.1002/pen.21210.
15. Chiang, C.R.; Ju, M.Y.; Chang, F.C. *Polym. Eng. Sci* **1998**, 38, 622.
16. Ju, M.Y.; Chang, F.C. *Polymer* **2000**, 41, 1719.
17. Miyata, T.; Masuko, T. *Polymer* **1998**, 39, 1399.

18. Kim, D.J.; KIM, W.S.; LEE, D.H.; Min, K.E.; Park, L.S.; Kang, I.K.; Jeon, I.R.; Seo, K.H. *J. Appl. Polym. Sci.* **2000**, 81, 1115.
19. Lumlong, S; Kuboyama, K; Chiba, T; Ougizawa, T. *Macromol. Symp.* **2006**, 233, 17.
20. Qui, Z.B.; Ikehara, T.; Nishi, T. *Polymer* **2003**, 44, 3095.
21. Yoo, E.S.; Im, S.S. *J. Polym. Sci.* **1999**, 37, 1357.
22. Yasiniwa, M.; Satou, T. *J. Polym. Sci.* **2002**, 40, 2411.
23. Al-Raheil, I.A.; Qudah, A.M.A. *Polym. Int.* **1995**, 37, 249.
24. Ichikawa, Y.; Noguchi, K.; Okyama, K.; Washiyama, J. *Polymer* **2001**, 42, 3703.
25. Ichikawa, Y.; Suzuki, J.; Washiyama, J.; Moteki, Y.; Noguchi, K.; Okuyama, K. *Polymer* **1994**, 35, 3338.
26. Ichikawa, Y.; Kondo, H.; Igarashi, Y,; Noguchi, K.; Okyama, K.; Washiyama, J. *Polymer* **2000**, 41, 4719.
27. Wang, R.; Wang, S.; Zhang, Y.; Wan, Z.; Ma, P. *Polym. Eng. Sci.* **2009**, 49, 26.

CHAPTER 4

Thermoplastic Vulcanizate based on Poly(lactic acid) and Acrylic Rubber Blend with Ethylene Ionomer

4.1 INTRODUCTION

TPEs prepared by dynamically vulcanized polymer blends, referred to as TPVs. TPVs consists of crosslinked rubber domain dispersed in thermoplastic matrix and are melt-reprocessable. To obtain TPVs with excellent properties, compatibility between the rubber and the thermoplastic is one of the most important factors. To improve compatibility and crosslinking of thermoplastic and rubber blend, some chemicals have been used to produce TPVs during melt-mixing. In an immiscible polymer blend, not only the chemical reaction but also the physical interaction is effective for compatibilize. For instance, ethylene ionomer has been sometimes used to compatibilize a polar polymer with a nonpolar polymer,[1] because the ionomer has both polar and non-polar components.

Acrylic rubber (ACM) is a vulcanizable, oil resistant and high temperature resistant rubber. ACM has been widely used in automotive seal, o-ling, gaskets, adhesives and so on.[2] It has low viscosity, and is commercialized with different types of cure-site monomers which can react with functional groups present in other polymers. We expected that the close viscosity between a thermoplastic and ACM may provide the fine morphology of the blend, because the viscosity ratio of component polymers is desirable to be around 1.0 to obtain the fine morphology.[3]

Poly(lactic acid) (PLA) is a biodegradable thermoplastic which shows high strength and stiffness, excellent transparency and biodegradability. Unfortunately, the brittleness of PLA prevents it from wide applications. Several reports have been performed for toughening of PLA by blending with rubbers.[4-7] However, not many studies have been reported on TPEs prepared using PLA,[8-9] and the TPE based on PLA/rubber blend by polymer blending with excellent properties has not been achieved so far, as for my knowledge.

4.1.1 Objective of this Chapter

In this research, new TPV was developed by melt-blending of PLA and ACM with ethylene ionomer as a compatibilizer. The crosslinking inside of the rubber phase was induced by addition of a crosslinking agent, and their morphology, properties and reaction were investigated.

4.2 EXPERIMENTAL

4.2.1 Materials

PLA with a trade name of Lacea was kindly supplied by Mitsui Chemicals Inc., which had melting point at 169 ^{o}C and molecular weight of 100,000. Detail of ACM was given in Chapter 3. Ethylene-methacrylic acid (EMAA) and EMAA ionomer having MAA content of 15% were kindly supplied from Dupont-Mitsui Polychemicals Co. Ltd. EMAA ionomer was partially neutralized by sodium ion (the degree of neutralization was 54%)(EMAA-Na). Hexamethylenediamine carbamate (HMDC) which acts as crosslinking agent of ACM was purchased from Wako Pure Chemical Industries, Ltd. The chemical structure of ACM is presented in Scheme 3.1 (Chapter 3), while PLA, HMDC and EMAA-Na are shown in Scheme 4.1, 4.2 and 4.3 respectively.

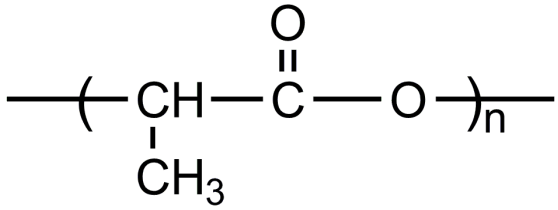

SCHEME 4.1. Chemical structure of PLA.

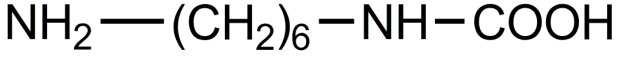

SCHEME 4.2. Chemical structure of HMDC.

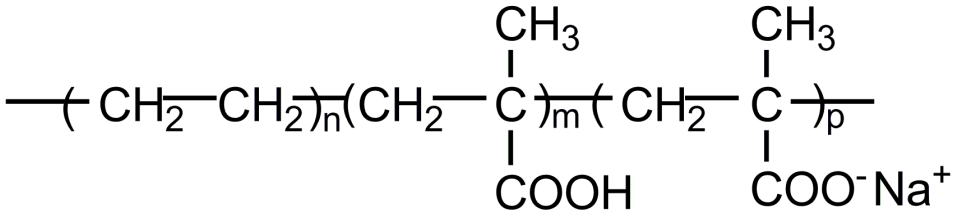

SCHEME 4.3. Chemical structure of EMAA-Na.

4.2.2 Sample Preparation

PLA was melt-mixed with ACM in compositions of 40/60 wt%/wt% at 210 ^{o}C for 10 min. EMAA or EMAA-Na (6 phr) was added to the blend as a compatibilizer. The sample was mixed at the rotation speed of 100 rpm using a twin screw compounder (DSM Xplore, Rheo Lab Ltd.). HMDC (1 and 4phr) was also added to the blend after melt-mixing of the blend for 5 min to induce the crosslinking in the ACM phase, and then continued to mix for 30 min.

4.2.3 Measurements

4.2.3.1 Tensile Properties Measurements

As given in Chapter 2.

4.2.3.2 Scanning Electron Microscopy (SEM)

SEM (SM-200, Topcon Corp.) was used to observe morphology of the blend. Cryo-fracuture surface of the blend was trimmed by a cryomicrotome equiped with a diamond knife at -80 ^{o}C, then rubber phase was removed from the cryo-fracture surface by toluene at room temperature. The trimmed cryo-fracture surface of the blend was sputter-coated with thin-layer of gold, and scanned with electron beam at an acceleration voltage of 10 kV.

4.2.3.3 *Transmission Electron Microscopy (TEM)*

Transmission electron microscopy (TEM, H-7650 Zero A, Hitachi High-Technologies Corp.) was used to record the morphology images of the blends at an acceleration voltage of 100 kV. Thin films were cryogenically sliced using a cryomicrotome equiped with a diamond knife at -80 ^{o}C and stained by ruthenium tetroxide vapor.

4.2.3.4 *Rheological Measurement*

As explained in Chapter 3.

4.2.3.5 *Differencial Scanning Calorimetry (DSC)*

The measurement was similar to that given in Chapter 2. Temperature range of DSC measurement was from -100 to 200 ^{o}C.

4.2.3.6 *Fourier Transform Infrared Spectroscopy (FTIR)*

The reaction between PLA, ACM and EMAA was investigated by FTIR (FT/IR-480 plus, Jasco Corp.). The samples were prepared by casting from their solutions (chloroform solutions for PLA and ACM; hot tetrahydrofuran solutions for EMAA and EMAA-Na). Solvent extraction technique was used to extract specific components in the blend for the measurement. EMAA-Na ionomer was extracted from the blended samples by stirring in chloroform at room temperature for 7 days to thoroughly remove the unreacted PLA and ACM, and then the extracted EMAA or EMAA-Na was dissolved in hot tetrahydrofuran. The solutions were spin-casted on silicon wafers, and dried in a vacuum oven at 60 ^{o}C for 12 h. IR spectra were measured in the range of 600 cm^{-1} to 4000 cm^{-1} with a resolution of 4 cm^{-1}.

4.3 RESULTS AND DISCUSSION

4.3.1 Mechanical Properties

Figure 4.1 shows tensile stress-strain curves of PLA/ACM blends. Figure 4.2 shows tensile hysteresis curves of them. Mechanical properties estimated from the stress-strain curves are listed in Table 4.1. The PLA/ACM blend showed yielding and poor strain recovery (35%). By addition of ionomer (EMAA-Na), tensile modulus hardly changed but tensile strength became low and strain at break was remarkably

improved from 189% to 870%. Moreover, recovery after stretching of 100% strain was also improved from 35% to 70%. In order to check the effect of Na^+ ion, a non-neutralized EMAA was also added to the PLA/ACM blend, and then only the strain at break was improved while the tensile modulus, the tensile strength and the strain recovery did not change. From the results, it was found that the EMAA-Na improved the mechanical properties of the PLA/ACM blends.

TABLE 4.1 Tensile properties of PLA, ACM and PLA/ACM blends.

Samples	Modulus (MPa)	Maximum tensile strength (MPA)	Strain at break (%)
PLA	4000	93	22
ACM	3.7	0.65	1200
PLA/ACM	273	3.5	189
PLA/ACM/EMAA	266	3.5	218
PLA/ACM/EMAA-Na	130	2.0	870

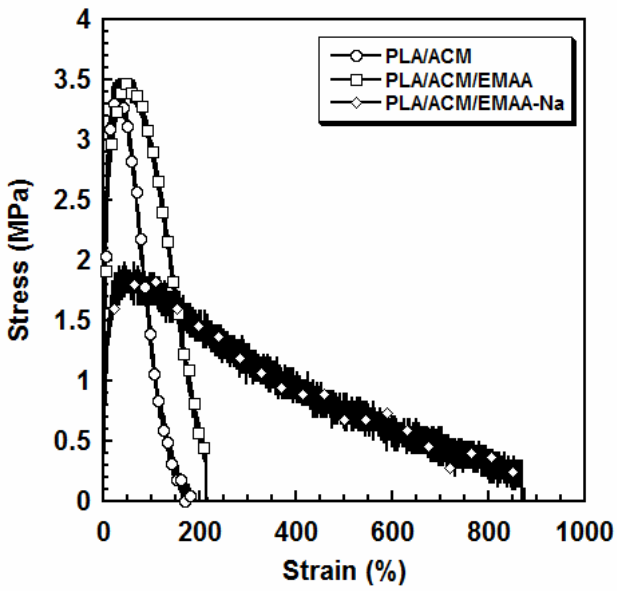

FIGURE 4.1 Stress-strain curves of PLA/ACM (40/60), PLA/ACM/EMAA (40/60/6) and PLA/ACM/EMAA-Na (40/60/6) blends.

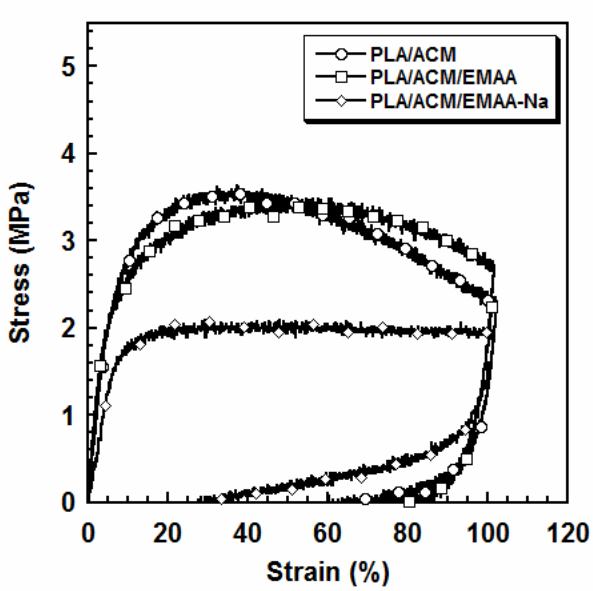

FIGURE 4.2 Strain recovery curves of PLA/ACM (40/60), PLA/ACM/EMAA (40/60/6) and PLA/ACM/EMAA-Na (40/60/6) blends.

4.3.2 Morphology

Since mechanical properties of polymer blends strongly depend on the morphology, the phase morphology of the PLA/ACM blends was observed by SEM and TEM. SEM image of cryo-fracture surface of the PLA/ACM blend of which the ACM was removed by solvent extraction, is shown in Figure 4.3. Because PLA does not react with ACM, the residual sample after solvent extraction was considered to be only PLA phase. The SEM image showed both some continuous space of which the removed ACM phase had existed and the continuous phase of PLA. Therefore, it was indicated that the PLA/ACM blend had co-continuous morphology. TEM images in Figure 4.4 further illustrated the phase structure of PLA binary and ternary blends. At first view, in the TEM image of PLA/ACM, ACM phase (dark region) looked to form continuous phase and PLA (bright region) was domain. However, the morphology of PLA/ACM blend was confirmed by the SEM image as co-continuous morphology. In PLA/ACM/EMAA and PLA/ACM/EMAA-Na blends, the blends was also expected to be co-continuous morphology similar to PLA/ACM blend by taking into account that the blends showed yielding in the tensile test. Figure 4.5 shows higher magnification TEM images of ACM rubber phase (dark region) and PLA phase (bright region) in PLA/ACM/EMAA-Na blend. In the ACM phase image (Figure 4.5 (a)), the darker particles with diameter of less than 50 nm were observed, while the particles were rarely observed in the PLA phase image (Figure 4.5 (b)). The nano-sized particles in the ACM

phase were considered to be EMAA-Na. From the results, it was considered that compatibility of EMAA-Na with ACM is higher than with PLA.

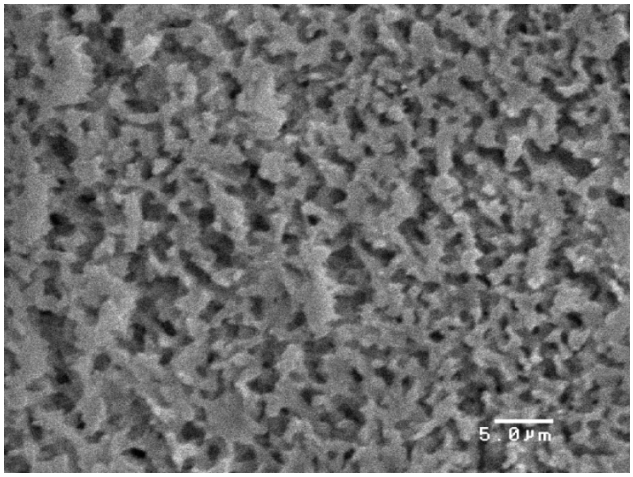

FIGURE 4.3 SEM image of cryo-fracture surface of PLA/ACM blend in which ACM was removed by toluene extraction.

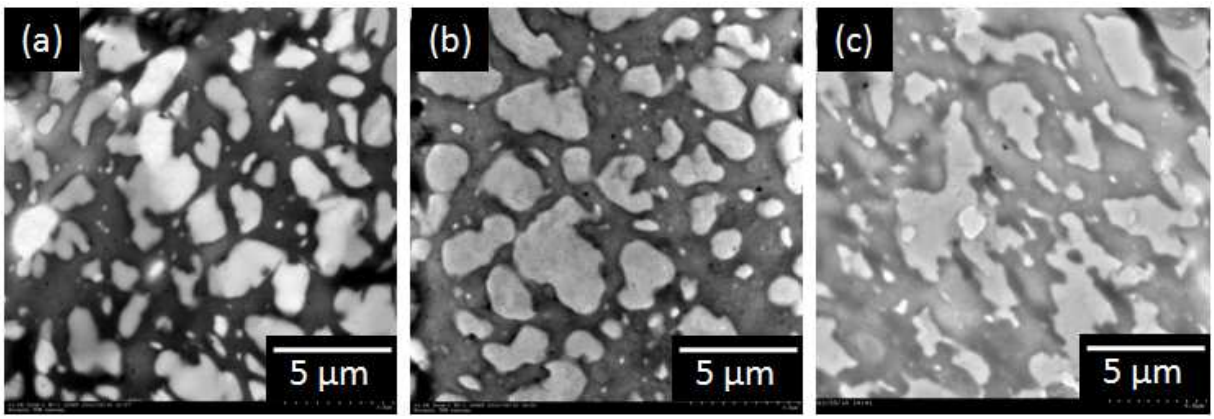

FIGURE 4.4 TEM images of (a) PLA/ACM, (b) PLA/ACM/EMAA and (c) PLA/ACM/EMAA-Na blends.

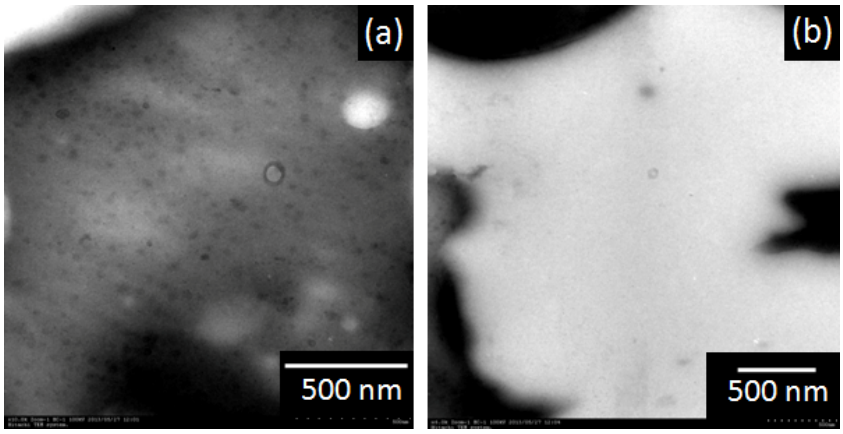

FIGURE 4.5 TEM images of (a) ACM phase and (b) PLA phase in PLA/ACM/EMAA-Na blend.

4.3.3 Rheological Properties

To demonstrate the reaction or the interaction between PLA, ACM and ionomer, the rheological measurement was employed. The complex viscosities of the PLA, EMAA, EMAA-Na, PLA/EMAA and PLA/EMAA-Na blends are plotted as a function of frequency at 210 ^{o}C in Figure 4.6. The complex viscosity of PLA slightly decreased with addition of EMAA, and decreased more in PLA/EMAA-Na (94/6) than in PLA/EMAA (94/6). The decreasing of complex viscosity in PLA/EMAA blend suggested chain scission of PLA under high melt-mixing temperature, and the result in a reduction of molecular weight that induced the decreasing of the complex viscosity. It

was reported that PLA easily degrades during melting process (e.g., via hydrolysis, depolymerization, oxidative and transesterification).[10] Since metal-ion in an ionomer is able to catalyze transesterification between polyesters,[1] the substantial decreasing of the complex viscosity of PLA/EMAA-Na indicated chain scission of PLA by metal-ion. The acceleration of chain scission rate of PLA by Na^+ ion has also been reported.[11] Figure 4.7 shows the plot of frequency dependence of complex viscosity of ACM, EMAA, EMAA-Na ionomer and ACM/EMAA and ACM/EMAA-Na binary blends. The complex viscosity of ACM/EMAA (94/6) and ACM/EMAA-Na (94/6) blends exhibited almost same behavior with ACM. This indicated that no chain extension and crosslinking reaction of ACM were occurred in the blend. Figure 4.8 shows the complex viscosity of PLA, ACM, binary blends of PLA/ACM and ternary blends of PLA/ACM/EMAA and PLA/ACM/EMAA-Na. In contrast with the binary blends of PLA and EMAA or EMAA-Na, the complex viscosity of the ternary blends increased by addition of EMAA-Na regardless of no reaction between EMAA-Na and ACM. These results suggested that the EMAA-Na acted as a compatibilizer between PLA and ACM because the viscosity of PLA/ACM increased by addition of EMAA-Na even though that of PLA decreased by addition of EMAA-Na.

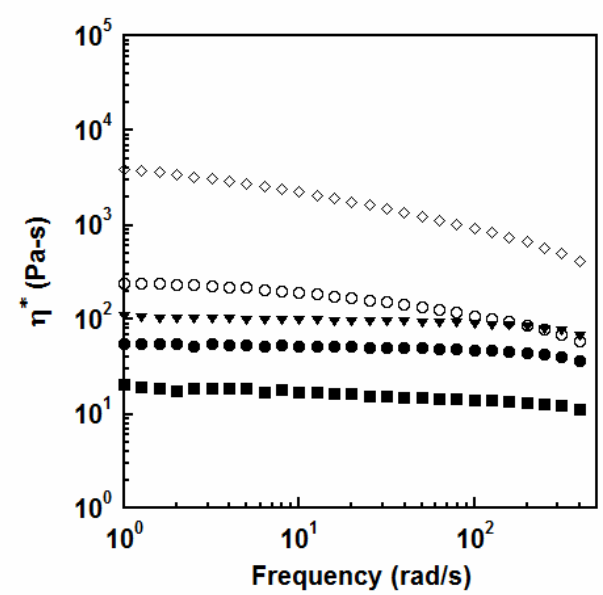

FIGURE 4.6 Frequency dependence of complex viscosity at 210 °C of (▼) PLA, (○) EMAA, (◇) EMAA-Na, (●) PLA/EMAA (94/6) and (■) PLA/EMAA-Na (94/6).

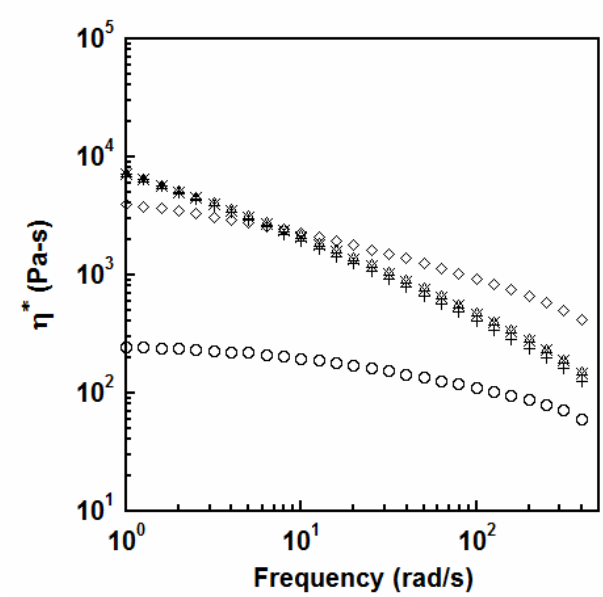

FIGURE 4.7 Frequency dependence of complex viscosity at 210 °C of (△) ACM, (○) EMAA, (◇) EMAA-Na, (×) ACM/EMAA (94/6) and (+) ACM/EMAA-Na (94/6).

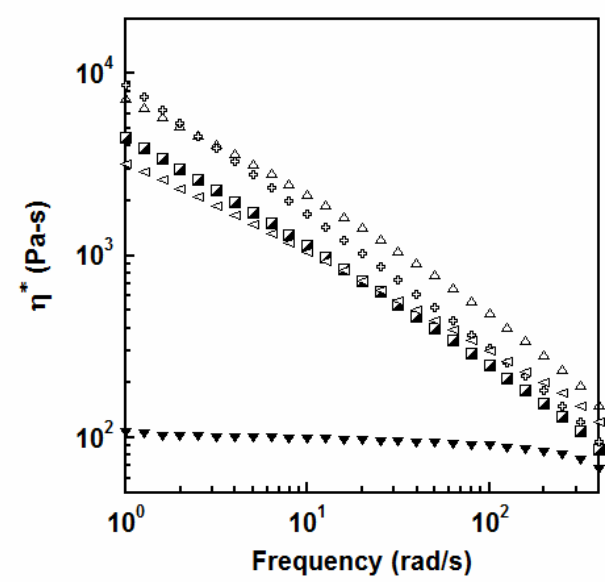

FIGURE 4.8 Frequency dependence of complex viscosity at 210 °C of (△) ACM, (▼) PLA, (◅) PLA/ACM (40/60), (◪) PLA/ACM/EMAA (40/60/6) and (✥) PLA/ACM/EMAA-Na (40/60/6).

4.3.4 Thermal Properties

Figure 4.9 shows DSC thermograms of PLA, ACM, PLA/ACM, PLA/ACM/EMAA and PLA/ACM/EMAA-Na blends. In PLA/ACM/EMAA-Na blend, glass transition temperature (T_g) of ACM appeared at the same temperature with pure ACM, while T_g and melting temperature (T_m) of PLA showed the decrease of 4 and 5 °C respectively. This T_g depression suggested the chain scission of PLA by EMAA-Na catalyst. The decreasing of T_m probably resulted from the increasing of interfacial

reaction between PLA and ACM by EMAA-Na catalyst, which induced smaller sizes of PLA crystal than pure PLA.

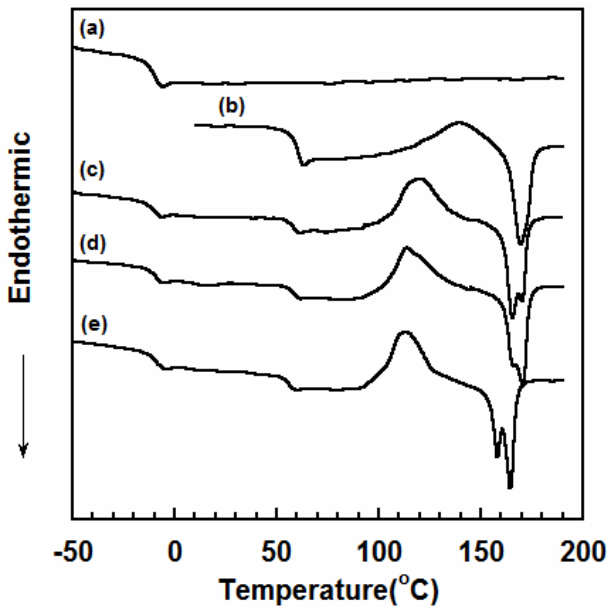

FIGURE 4.9 DSC heating scans at 10 ^{o}C min^{-1} of (a) ACM, (b) PLA, (c) PLA/ACM, (d) PLA/ACM/EMAA and (e) PLA/ACM/EMAA-Na.

4.3.5 Reaction Mechanism

Figure 4.10 shows FTIR absorption spectra of PLA, ACM, EMAA-Na and EMAA-Na phase solvent-extracted from PLA/ACM/EMAA-Na. From the results, absorption peak due to stretching vibration of carbonyl group (C=O) of PLA, ACM and EMAA appeared at 1756, 1733 and 1700 cm^{-1} respectively.[1,12,13] Absorption peaks

assigned to C-O-C vibration were observed at 1187 and 1105 cm^{-1} in PLA,[12] while at 1116 and 1248 cm^{-1} in ACM.[13] These C-O-C peaks were not observed in EMAA-Na. In PLA/ACM/EMAA and PLA/ACM/EMAA-Na ternary blends, unreacted PLA and ACM were removed by chloroform extraction, and then residual EMAA-Na phase in the blends was measured by FTIR. The extracted EMAA-Na phase in PLA/ACM/EMAA-Na blend showed C=O peaks of ACM and EMAA-Na and small shoulder peak of PLA around 1730 cm^{-1}. In addition, the C-O-C peak at 1105 cm^{-1} was observed, while the other C-O-C peak was very week. These results indicated that some of PLA and ACM also extracted with EMAA-Na, and the fact suggested that there were reaction between them. To check the interaction between EMAA-Na and PLA or ACM, FTIR spectra of solvent extracted EMAA-Na phases in PLA/EMAA-Na and in ACM/EMAA-Na binary blends and extracted PLA phase in PLA/ACM blend were measured as shown in Figure 4.11. PLA phase of PLA/ACM presented almost same spectra with pure PLA, and this means that there was no reaction between PLA and ACM in the PLA/ACM binary blend. EMAA-Na phase of the ACM/EMAA-Na blend showed apparent C=O peak of ACM (1733 cm^{-1}), while that of the PLA/EMAA-Na blend at 1755 cm^{-1} was very weak. It was suggested that EMAA-Na interacted with carboxylic end group of PLA and reacted with epoxy group of ACM by carboxyl group of EMAA-Na. EMAA-Na phase of PLA/ACM/EMAA-Na ternary blend represented C-O-C peak at 1105 cm^{-1}, while not in the PLA/EMAA-Na and ACM/EMAA-Na binary

blends. Therefore, the C-O-C peak in EMAA-Na phase of PLA/ACM/EMAA-Na did not come from the interaction between PLA and EMAA-Na or the reaction between ACM and EMAA-Na. Liu *et al*. have also been reported that EMAA neutralized by metal-ion can improve interfacial adhesion between PLA and a rubber containing epoxy group by the improving of interfacial reaction, because the metal-ion in EMAA ionomer can act as an initiator and catalyst to accelerate reaction between carboxylic end group of PLA and epoxy group of rubber.[1,15] It is known that epoxy can react with both carboxyl and hydroxyl groups to form ester and ether linkages under suitable conditions, respectively, while the reaction with carboxyl group has higher reactivity than the reaction with hydroxyl group.[1] It was indicated that the detected C-O-C peak at 1105 cm^{-1} in EMAA-Na phase of PLA/ACM/EMAA-Na blend originated from the interfacial reaction between carboxylic end group of PLA and epoxy group of ACM, which was accelerated by catalytic effect of metal ion in EMAA-Na.

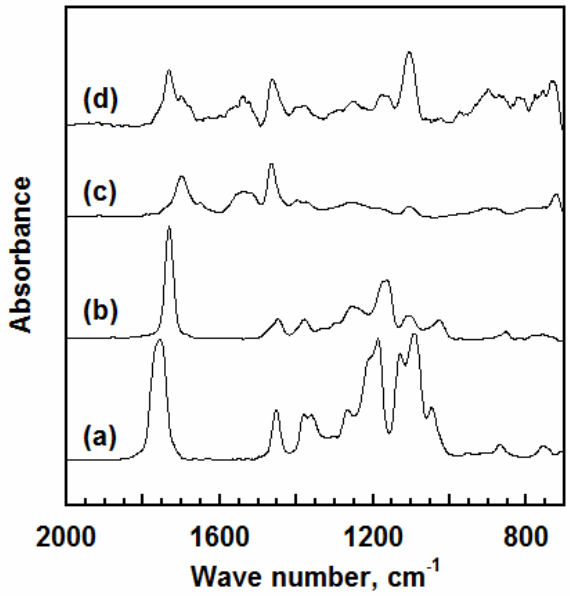

FIGURE 4.10 FTIR spectra of (a) PLA, (b) ACM, (c) EMAA-Na and (d) EMAA-Na phase of PLA/ACM/EMAA-Na.

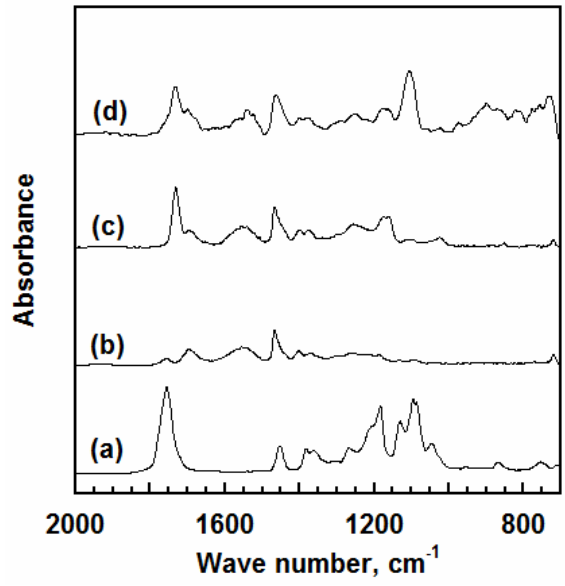

FIGURE 4.11 FTIR spectra of (a) PLA phase of PLA/ACM, (b) EMAA-Na phase of PLA/EMAA-Na, (c) EMAA-Na phase of ACM/EMAA-Na and (d) EMAA-Na phase of PLA/ACM/EMAA-Na.

4.3.6 Influence of Crosslinking

Although the tensile properties of PLA/ACM blend were improved by addition of ethylene ionomer as described before, the obvious yielding was still observed even in the ternary blend. Li et al. reported that mechanical properties of PVDF/ACM blend were improved via the dynamic vulcanization by addition of HMDC.[15] Therefore, to improve the drawback of PLA/ACM/EMAA-Na blend described above, ACM phase in the ternary blend was dynamically vulcanized by addition of HMDC during the mixing process. Figure 4.12 shows tensile stress-strain curves of 0, 1, and 4 phr of HMDC added PLA/ACM/EMAA-Na blends and PLA/ACM with HMDC 4 phr. By addition of 1 phr of HMDC, the PLA/ACM/EMAA-Na blend also showed the yielding, however, the stress hardly decreased after the yielding, while the PLA/ACM/EMAA-Na blend without HMDC showed decrease of the stress. This was considered to originate in the chemical crosslinking formation in the rubber phase by HMDC. By addition of more amount of HMDC (4 phr), the PLA/ACM/EMAA-Na blend showed the decreasing of modulus and the apparent yielding was not observed. To clarify whether the primary factor for the behavior was crosslinking formation or not, PLA/ACM blend with 4 phr of HMDC was also prepared and tensile test was performed. As the result, the stress after yielding showed decrease in contrast with PLA/ACM/EMAA-Na with 4 phr HMDC. Strain recovery curves of the blends were presented in Figure 4.13. In the blend of PLA/ACM/EMAA-Na with 4 phr of HMDC, the strain recovery was improved about

10% than that without crosslinking of ACM rubber. However, the improvement of recovery was not observed in PLA/ACM blend with addition of HMDC 4 phr. This indicated that both EMAA-Na and HMDC was necessary for improvement of mechanical properties of the blend. By melting the PLA/ACM/EMAA-Na with 4 phr of HMDC at the higher temperature than the melting temperature of PLA, this blend could be molded more than 4 times, that is, it was confirmed that this blend was reprocessable. From the results, it was obvious that the addition of HMDC into the PLA/ACM/EMAA-Na blend was effective for the improving the mechanical properties of the PLA/ACM/EMAA-Na blend as TPE.

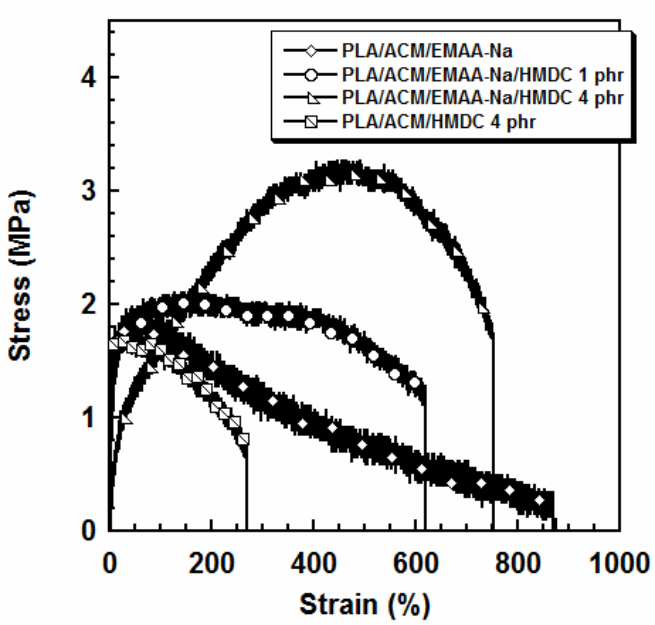

FIGURE 4.12 Stress-strain curves of PLA/ACM/EMAA-Na, PLA/ACM/EMAA-Na with 1 phr of HMDC, PLA/ACM/EMAA-Na with 4 phr of HMDC and PLA/ACM with 4 phr of HMDC.

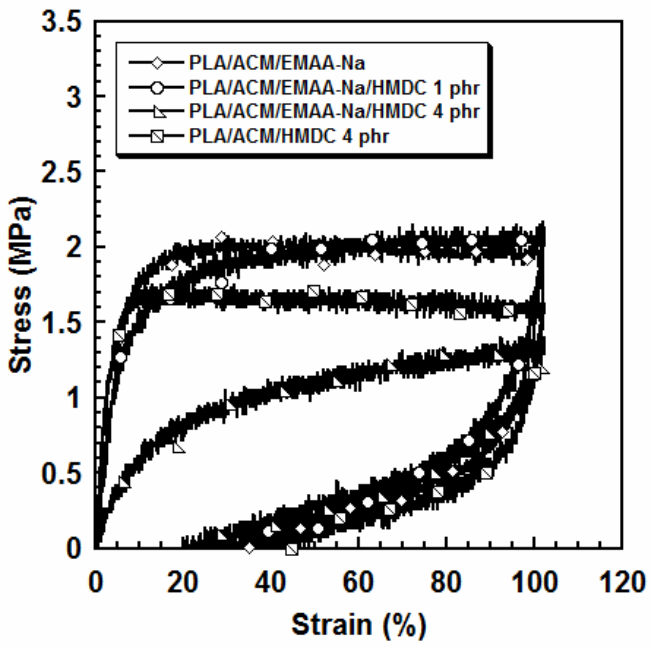

FIGURE 4.13 Strain recovery curves of PLA/ACM/EMAA-Na, PLA/ACM/EMAA-Na with 1 phr of HMDC, PLA/ACM/EMAA-Na with 4 phr of HMDC and PLA/ACM with 4 phr of HMDC.

Figure 4.14 shows TEM images of PLA/ACM/EMAA-Na blend with 1 and 4 phr of HMDC. The blend with 1 phr of HMDC showed continuous ACM rubber phase (dark region) and PLA phase (bright region) with large distribution of the thickness from a few tens nanometers to several micrometers as shown in Figure 4.14(a). In contrast with it, it was found that the blend with 4phr of HMDC showed connecting spherical rubber particles with diameter of about 1μm form continuous phase (dark region) and the thickness of PLA phase (bright region) was relatively uniform as shown in Figure 4.14(b), that is, about 500 nm which was considered to be also continuous phase.

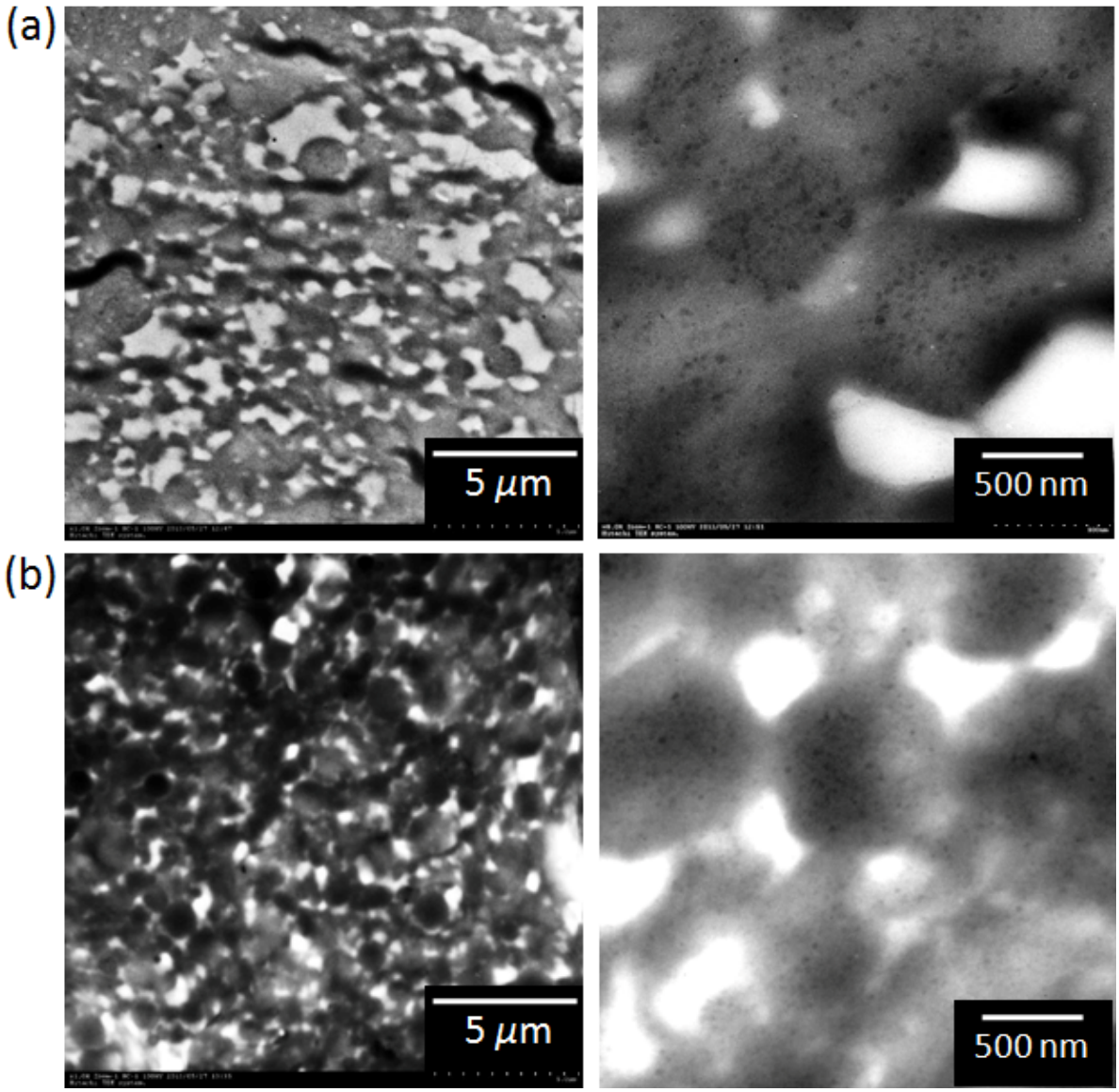

FIGURE 4.14 TEM images of (a) PLA/ACM/EMAA-Na with 1 phr of HMDC and (b) with 4 phr of HMDC.

In order to check the polymer component forming the continuous phase in the blends, the ternary blend with 4 phr of HMDC was immersed into chloroform which is good solvent for both PLA and ACM. The result is shown in Table 4.2 and those for the

PLA/ACM blends without HMDC and without EMAA-Na were also shown as reference. It was found that both blends of PLA/ACM/EMAA-Na with and without 4 phr of HMDC swelled, while both blends of PLA/ACM with and without 4 phr of HMDC dissolved in chloroform. By FTIR measurement of the dried film of extracted solution and the dried gel, it was confirmed that PLA and small amount of ACM was dissolved into chloroform and the gel consisted of ACM phase. From the result and the fact that the blend showed much high modulus than ACM rubber, it was suggested that the PLA also form continuous phase, that is, the blend had co-continuous phase morphology. Moreover, when the gels in chloroform were shaken, they broke and finely dispersed into chloroform. For comparison, 4 phr of HMDC added ACM was also immersed into chloroform and the chemically crosslinked ACM gel was also swelled, however, it did not break by shaking it. As described before, it was suggested that there was chemical reaction between epoxy group of ACM and carboxylic acid of EMAA-Na in the PLA/ACM/EMAA-Na blend. However, the fact that the gel easily broke and finely dispersed into chloroform indicated the major crosslinking point was physical one. By taking account that the ionomer formed ionic aggregates, it was considered that the aggregates acted as the crosslinking points in the gel.

TABLE 4.2 Swelling test in chloroform of PLA/ACM, PLA/ACM/EMAA-Na, PLA/ACM/HMDC and PLA/ACM/EMAA-Na/HMDC

Sample	Condition	After shaking
PLA/ACM (40/60)	Dissolved	-
PLA/ACM/HMDC (40/60/4)	Dissolved	-
PLA/ACM/EMAA-Na (40/60/6)	Swelled	finely dispersed
PLA/ACM/EMAA-Na/HMDC (40/60/6/4)	Swelled	finely dispersed

On the basis of all above results, the plausibly possible model of phase morphology of the PLA/ACM/EMAA-Na blend with 4 phr of HMDC is proposed as shown in Figure 4.15.ACM rubber particles with diameter of about 1μm were connected each other and formed the continuous phase in the blend. The ethylene ionomer mainly dispersed in the ACM particles homogeneously. Such morphology might be formed as follows: The small ACM particles were formed due to crosslinking by addition of HMDC because coalescence of the broken particles during melt-mixing was restricted by the crosslinking formation in the rubber particles. The connecting of particles might be induced by both chemical reaction between ACM and ionomer, and ionic aggregate formation of ionomer in the ACM phase. From the fact that the gel of the blend in chloroform finely dispersed by shaking the solution, major reasons of the connection were the physical interactions. On the contrary, in the PLA/ACM blend with

4 phr of HMDC, the physical crosslinking could not be formed due to the lack of EMAA-Na, it was considered that the blend dissolved into chloroform. In the PLA/ACM/EMAA-Na with 4 phr of HMDC, connection of small and uniform sized rubber particles might provide the thinner PLA phase, and this must be the reason of good mechanical properties, because the thin plastic phase could deform at lower stress.

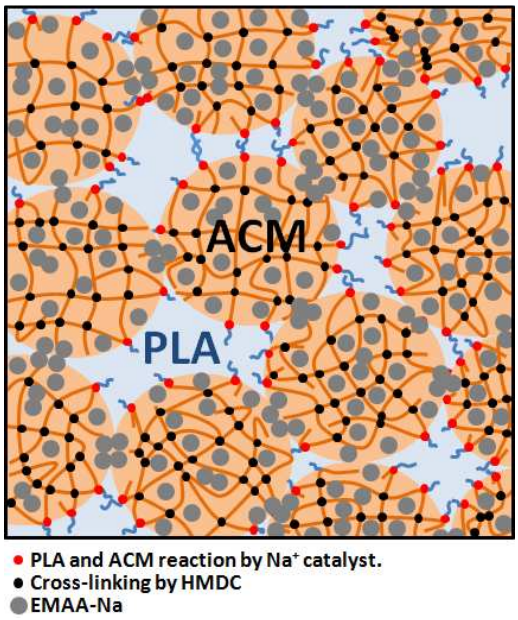

FIGURE 4.15 The plausibly possible model of PLA/ACM/EMAA-Na/HMDC blend.

4.4 CONCLUSIONS

New biodegradable TPV was successfully developed with the excellent tensile strength at break and strain recovery by the melt-blending process of

PLA/ACM/EMAA-Na/HMDC. SEM and TEM images revealed that phase inversion occurred from co-continuous morphology to the dispersed ACM domain in PLA matrix by addition of 4 phr of HMDC due to higher crosslinking. Elastic recovery and tensile strength at break of PLA/ACM/EMAA-Na/HMDC blend were improved by addition of EMAA-Na and HMDC. PLA/ACM/EMAA-Na/HMDC blend was confirmed to be a good TPV because it showed excellent strain recovery and reprocessing ability. Na^+ ion in EMAA-Na was found to improve interfacial reaction through end group of PLA and epoxy group of ACM because Na^+ ion acted as a catalyst to accelerate the interfacial reaction. From the results, the possible plausible model for the blend was proposed that the co-continuous phase was formed with both the mainly physically connected spherical rubber particles with uniform diameter and surrounding thin PLA phase. The physical connection of the spherical particles might be due to ionic aggregate formation in and between ACM particles. By adopting the model of fine morphology, both the reprocess ability and the excellent mechanical properties could be explained.

4.5 REFERENCES

1. Lui, H.; Chen, F.; Lui, B.; Estep,G.; Zhang, J. *Macromolecules***2010**, 43, 6058.
2. Soares, B. G.; Santos, D. M.; Sirqueira, A. S. *Express Polym. Lett.* **2008**, 2, 602.
3. Wu, S. *Polym. Eng. Sci*. **1987**, 27, 335.

4. Ishida, S.; Nagasaki, R.; Chino, K.; Dong, T.; Inoue, Y. *J. Appl. Poly. Sci*. **2009**, 113, 558.
5. Li, Y.;Shimizu, H. *Macromol. Biosci*. **2007**, 7, 921.
6. Anderson, K. S.; Lim, S.H.; Hillmyer, M.A. *J. Appl. Polym. Sci*. **2003**, 89, 3757.
7. Rahul M. R.; Douglas E. H. *Macromol. Mater. Eng.***2010**, 295, 204.
8. Kim, J.H.; Lee, J.H. *Polym. j.***2002**, 34, 203.
9. Cohn, D.; Hotovely S. A. *Biomaterials,* **2005**, 26, 2297.
10. Sodergard, A.; Stold, M. *Prog.Polym. Sci.***2002**, 27, 1123.
11. Han, S., I.; Yoo, Y.; Kim, D. K.; Im, S. S. *Macromol. Biosci.***2004**, 4, 199.
12. Yang, S. L.; Wu, Z. H.; Yang, W.; Yang, M. B. *Polym. Test.***2008**, 27, 957.
13. Jha, A.; Bhowmick, A, K.; Fujitsuka, R.; Inoue, T. *J. Adhesion Sci. Technol.***1999**, 13, 649.
14. Lui, H.; Song, W.; Chen, F.; Guo, L.; Zhang, J. *Macromolecules***2011**, 44, 1513.
15. Li, Y.; Oono, Y.; Kadowaki, Y.; Inoue, T.; Nakayama, K.; Shimizu, H. *Macromolecules***2006**, 39, 4195.
16. I'Abee, R. M. A.; Duin, M. V.; Spoelstra, A. B.; Goossens, J. G. P. *Soft. Matter.* **2010**, 6, 1758.

CHAPTER 5

Thermoplastic Elastomer by Terpolymer Reactive Blending of Polyamide, Ethylene-1-Butene Rubber and Ionomer

5.1 INTRODUCTION

Thermoplastic elastomers prepared by blending of thermoplastic and rubber have gained considerable interest due to both its ease in melt-processing like thermoplastic and elasticity like rubber. Ideal morphology of such blends is the finely dispersed rubber particles in the thermoplastic matrix. Compatibility and adhesion between the thermoplastic and the rubber are two of the most important factors which control the overall TPE's performance. Reactive blending is one of the methods to improve the compatibility between two immiscible polymers in a blend. It is reported that chemical reaction between the thermoplastic and the rubber phases is effective to increase the interfacial adhesion between two polymers.[1,2] By introducing a reactive group which can react with one of the component polymers into the other one, graft or block copolymers of the polymers are formed during melt-mixing process. As the reactive group, amino,

hydroxyl, carboxyl, epoxy or maleic anhydride (MAH) groups have been used to form the copolymer at the interface and improve the compatibility, which leads to fine and homogeneous morphology, improvement of interfacial adhesion, and so on.[3-7] In addition, some reports employed ethylene-methacrylic acid (EMAA) ionomer neutralized by metal ion as a compatibilizer of a polymer blend because it is comprised of both polar and non-polar components.[8]

It is also known that dynamic vulcanization is effective methods to improve the mechanical properties of TPE based on polymer blend by crosslinking the rubber phase during melt-mixing process.[3] In this way, the crosslinking point formation in the rubber phase is important factor for the mechanical properties of TPE. Although the crosslinking points formed by the dynamic vulcanization is chemical ones, physical crosslinking points can be also effective to the mechanical properties of TPE. For example, in the ionomer, the ionic aggregates by neutralization of acid groups act as physical crosslinking points. The number of the aggregates depends on the neutralization degree, and the mechanical properties of the ionomer are also affected by them. The ionic groups tend to form ionic bond leading to ionic aggregates in the ionomer,[9-11] and the interaction is expected to improve the compatibility or to form physical crosslinking points in immiscible polymer blends.

Many TPEs prepared so far have poor heat resistance. For example, polypropylene (PP)/ethylene-propylene diene terpolymer, PP/natural rubber, PP/nitrile

rubber and so on have an allowable upper temperature limit at 160 ^{o}C.[12] The heat resistance of TPE can be enhanced by using a thermoplastic with high melting point.[13] The other problems of TPE also are oil and solvent resistance. To overcome the problems, Jha et al. reported the development and properties of heat- and oil-resistant TPE from polyamide-6 (PA6) and acrylate rubber (ACM) blends.[4] Effect of chemical reaction to adhesion between amino end group of PA6 and epoxy group of ACM has also been reported.[5]

5.1.1 Objective of this Chapter

In this research, a novel heat- and oil-resistant TPE based on PA6 and ethylene-1-butene (EB) blend was investigated. EB are selected because this rubbers is valuable for their excellent resistance to heat, oxidation, ozone and weather aging due to their stable, saturated polymer backbone structure. To compatibilize the blend, MAH grafted EB (EB-*g*-MAH) was also used as rubber component and EMAA ionomer neutralized by sodium ion (EMAA-Na) was added to the blend. As for our knowledge, this work is the first research to study on the effect of ionomer in TPE based on PA6/rubber blend. The ionomer may play the important role to improve properties of the blend. Then, the mechanical properties, morphology, rheological behavior, interfacial adhesion were studied.

5.2 EXPERIMENTAL

5.2.1 Materials

PA6 with a trade name of Novamid 1010J was kindly supplied by Mitsubishi Engineering-Plastics Corp., of which molecular weight was 16,400. Ethylene-1-butene copolymer (EB) and maleic anhydride grafted ethylene-1-butene copolymer (EB-*g*-MAH) (1-butene content = 20 wt% and MAH content = 2wt%) were kindly supplied by Mitsui Chemicals, Inc. Ethylene-methacrylic acid ionomer (EMAA) (MAA content was 15wt%) and ethylene-methacrylic acid ionomer with sodium ion (EMAA-Na) (MAA content was 15wt% and neutralization degree of sodium was 54%) were kindly supplied from Dupont-Mitsui Polychemicals Co. Ltd. The chemical structure of EB-*g*-MAH and EMAA-Na are presented in scheme 2.3 (in Chapter 2) and 3.3 respectively (in Chapter 3), while PA6 and is shown in scheme 5.1.

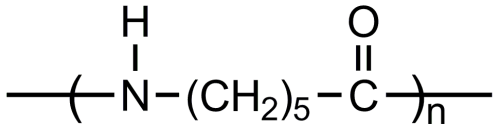

SCHEME 5.1 Chemical structure of PA6

5.2.2 Sample Preparation

Binary blends of PA6/EB and PA6/EB-*g*-MAH were melt-blended in compositions of 40/60 wt%/wt%, while ternary blends of PA6/EB-*g*-MAH/EMAA-Na was blended with 38/60/2 wt%/wt%/wt% at 250 ^{o}C for 10 min. The mixing was

performed at rotation speed of 100 rpm using a twin screw compounder (DSM Xplore, Rheo Lab Ltd.).

5.2.3 Measurements

5.2.3.1Tensile Properties Measurements

As given in Chapter 2.

5.2.3.2Morphological Analysis

Transmission electron microscopy (TEM) was explained in Chapter 4.

5.2.3.3 Measurement of adhesive energies

The interfacial fracture toughness (G_c) between the polymers used in this study was measured by asymmetric double cantilever beam (ADCB) method to estimate the interfacial adhesion.[14] Samples for ADCB test were prepared as shown in Figure 5.1.PA6 and EMAA-Na sheets with 1 mm thickness were prepared by the compression molding at 250 and 200^{o}C respectively. The films of EB and EB-g-MAH with 1 μm were prepared by spin-coating from toluene solution of 2 wt% onto the PA6 and the EMAA-Na sheets. Then, the spin-coated films on the sheets were dried under vacuum at 50 ^{o}C for 24 h. The polymer sheets and the films on the sheets were cut into a strip with dimension of 5.0 x 0.5 x 0.1 cm. One of the sheets was put on top of the spin-coated film and then the specimens with three layers were annealed for 0.5 h at 200 ^{o}C (PA6

sheet) and 70 ^{o}C (EMAA-Na sheet) respectively. The annealed three layered sample was placed on a glass plate, and then a razor blade of thickness 0.25 mm was pushed into the sandwich specimen along the interface of upper sheet and a spin-coated film until it reached 1 cm from the edge of a sample. The yield crack length between the edge of the blade and the crack tip was measured by optical microscope, after that the blade was pushed in again by 0.5 cm. This process was repeated three times and the crack length data was averaged. The G_c was then calculated by the following equation:[14]

$$G_c = \frac{3Ed^3b^2}{8a^4[1+(0.64d/a)]^4} \qquad (5.1)$$

Where E is Young's modulus of PA6 (1.2 GPa) and EMAA-Na (153 MPa), a is the crack length, b and d are the thickness of the razor blade and the upper sheet respectively.

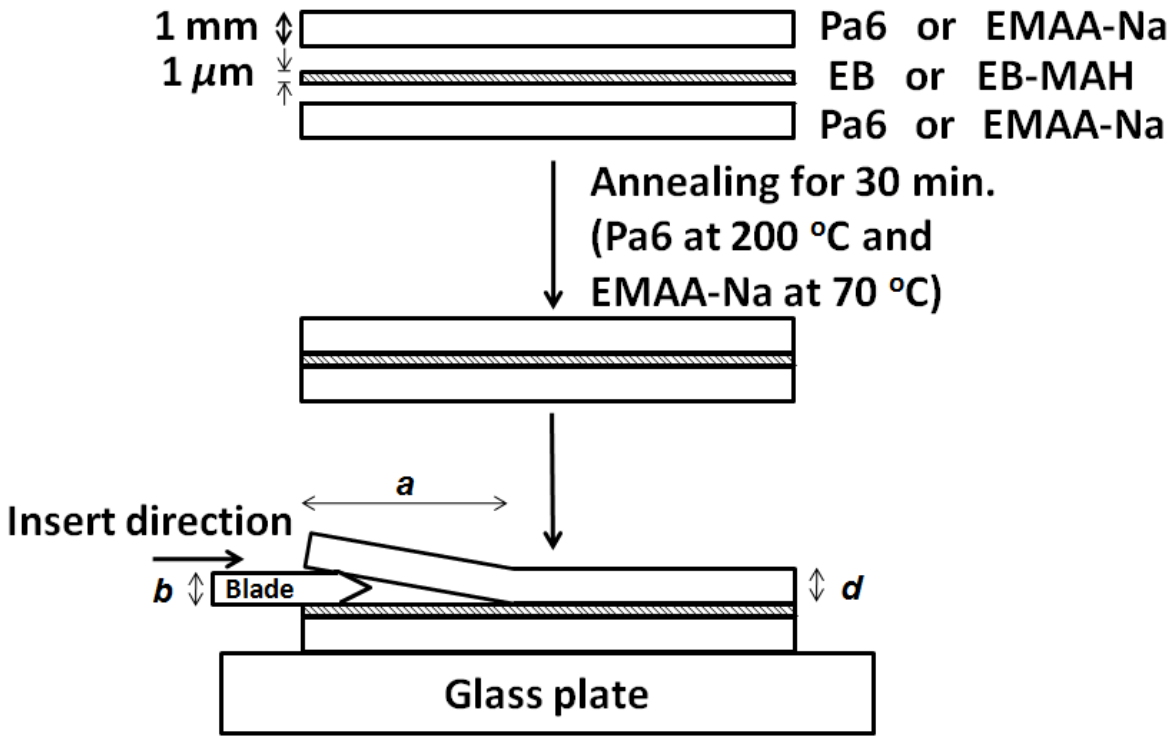

FIGURE 5.1 Sample preparation for ADCB method.

5.2.3.4 Rheological Measurement

As explained in Chapter 3.

5.2.3.5 Fourier Transform Infrared Spectroscopy (FTIR)

As described in Chapter 2.

5.3 RESULTS AND DISCUSSION

5.3.1 Mechanical Properties

Figure 5.2 shows tensile stress-strain curves of PA6, PA6/EB (40/60 wt%/wt%), PA6/EB-*g*-MAH (60/40) and PA6/EB-*g*-MAH/EMAA-Na (38/60/2) blends. Tensile properties estimated from the tensile measurement are listed in Table 1. PA6/EB-*g*-MAH blend showed the improvement of elongation at break and the decrease of Young's modulus compared to PA6/EB blend. Moreover, PA6/EB-*g*-MAH/EMAA-Na blend showed the increase in tensile strength at break with high elongation at break. Strain recovery test was also performed for the samples as shown in Figure 5.3. PA6 showed poor strain recovery of about 10%, while PA6/EB blend broke below 100% of strain. PA6/EB-*g*-MAH blend exhibited recovery of 75% similarly to elastic materials, and PA6/EB-*g*-MAH/EMAA-Na blend also presented the same recovery with PA6/EB-*g*-MAH blend. From the result, it was suggested that the maleic anhydride effectively worked on compatibilizing the blend, while the compatibility of PA6 and EB was not good.

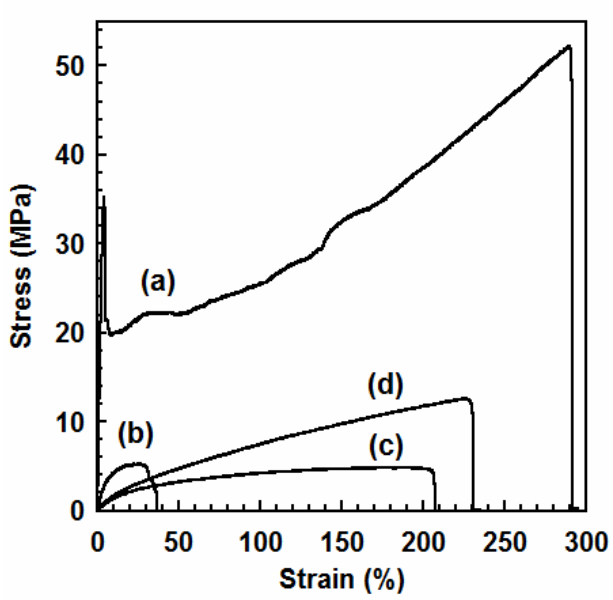

FIGURE 5.2 Stress-strain curves of (a) PA6, (b) PA6/EB (40/60), (c) PA6/EB-g-MAH (40/60) and (d) PA6/EB-*g*-MAH/EMAA-Na (38/60/2) blends.

TABLE5.1 Tensile properties of samples.

Samples	Young's modulus (MPa)	Tensile strength (MPa)	Tensile strain at break (%)	Strain recovery (%)
PA6	1,200	52	280	10
PA6/EB	59	5.2	37	-
PA6/EB-*g*-MAH	14	4.3	205	75
PA6/EB-*g*-MAH/EMAA-Na	18	12.6	230	73

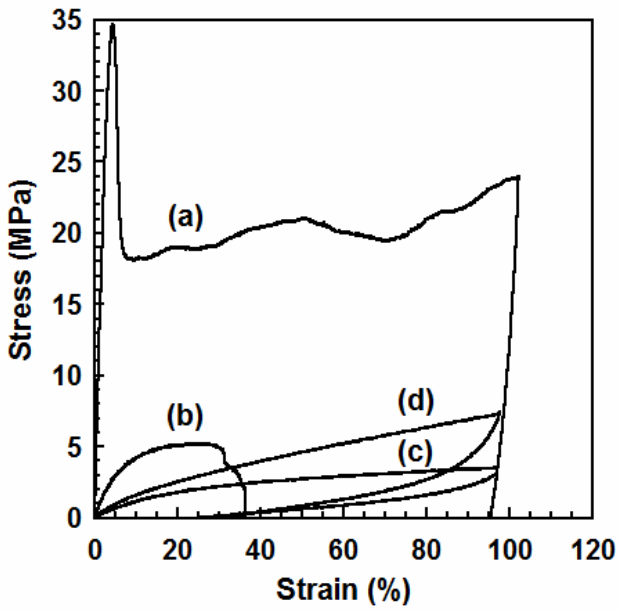

FIGURE 5.3 Strain recovery curves of (a) PA6, (b) PA6/EB (40/60), (c) PA6/EB-*g*-MAH (40/60) and (d) PA6/EB-*g*-MAH/EMAA-Na (38/60/2) blends.

5.3.2 Morphology

TPE made by blend should have the morphology of sea-island structure in which the matrix phase is a thermoplastic and the dispersed phase is a rubber. To check the blend morphology, TEM observation was performed to the samples. Figure 5.4 shows TEM images of the PA6/EB, PA6/EB-*g*-MAH (40/60) and PA6/EB-*g*-MAH/EMAA-Na (38/60/2) blends. As shown in Figure 5.4(a), the matrix phase of PA6/EB blend was EB (dark region) and the dispersed phase was PA6 (bright region). Phase inversion from EB matrix to the dispersed EB domain in PA6 matrix was observed by MAH modification of EB, and the morphology became extremely finer [Figure 5.4(b)]. This suggests that

the compatibility between the two component polymers was remarkably improved. The reaction of amino end group of PA6 with MAH grafted on a polymer have been reported.[15-19] Moreover, Charoensirisomboon et al. also reported that phase inversion of a polyamide blend was induced by an interfacial reaction.[20] From the reports, it was suggested that copolymer of PA6 and EB-*g*-MAH was formed at the interface by the reaction between amino end group of PA6 and MAH of EB-*g*-MAH during melt-mixing process.

PA6/EB-*g*-MAH/EMAA-Na blend (Figure 5.4c) exhibited the similar morphology with PA6/EB-*g*-MAH. The EMAA-Na phase should be also observed as dark region by the ionic aggregates. However the rubber particles finely dispersed into the PA6 matrix, that is, both the particle size and the inter-particle distance were less than 40 nm, and then in PA6/EB-*g*-MAH/EMAA-Na blend, it was hard to distinguish the EMAA-Na phase from the rubber phase in the TEM image. In addition, PA6/EB-*g*-MAH/EMAA-Na blend showed the increase of tensile strength at break, while the morphology of PA6/EB-*g*-MAH was very similar with PA6/EB-*g*-MAH/EMAA-Na. Therefore, it is considered that the increase in tensile strength at break of PA6/EB-*g*-MAH/EMAA-Na blend was not due to the morphology difference but some kind of crosslink in the rubber phase.

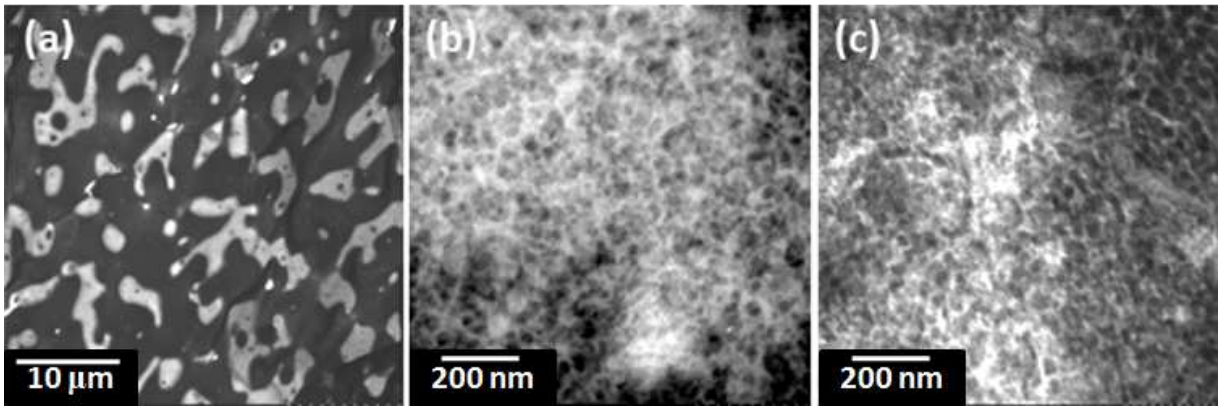

FIGURE 5.4 TEM images of (a) PA6/EB, (b) PA6/EB-*g*-MAH and (c) PA6/EB-*g*-MAH/EMAA-Na blends.

5.3.3 Adhesion between Component Polymers

To estimate the adhesion between the component polymers, the fracture toughnesses, G_c, between pairs of polymers used in this study were estimated by ADCB method as shown in Table 2, which is an indicator of the adhesion strength. G_c data exhibited that PA6 showed extremely high interfacial adhesion strength with EB-*g*-MAH, while it did low strength with EB and EMAA-Na. In the case between PA6 and EB-*g*-MAH, it was expected that copolymer was formed by the reaction between amino end group of PA6 and MAH of EB-*g*-MAH at the interface, and in fact, the reaction between MAH group grafted onto a polymer and amino end group of PA6 has been reported.[21-23] By contrast with it, in the case between PA6 and EB or PA6 and EMAA-Na, no copolymer formation was expected, and they showed much lower interfacial

adhesion than that between PA6 and EB-*g*-MAH. In the case of adhesion between EMAA-Na and EB-g-MAH, the adhesion strength was relatively high, although the chemical reaction was not expected between them. This fact suggested that there was some sort of attractive interaction between them.

Table 5.2 Fracture toughness, G_c between two polymers by ADCB method.

Samples	PA6/EB	PA6/EB-*g*-MAH	PA6/EMAA-Na	EMAA-Na/EB-*g*-MAH
G_c (J/m^2)	39	490	11	86

Because the adhesion between the component polymers in the melt state during mixing process affects the morphology of the blend, complex melt viscosity (η^*) at 250 ^{o}C of the neat polymers and the blended samples were measured as shown in Figure 5.5. PA6/EMAA-Na (90/10) blend and PA6/EB (40/60) blend represented the values between neat polymers. PA6/EB-*g*-MAH blend showed the increasing of η^* at low frequency compared to PA6/EB, and PA6/EB-*g*-MAH/EMAA-Na blend showed higher viscosity than that of each component polymer. It was considered that the increase in η^* of PA6/EB-*g*-MAH blend (Figure 5.5) was due to the reaction between amino end groups of PA6 and MAH groups of EB-*g*-MAH. As shown in Figure 5.6, η^* of EMAA/EB-*g*-MAH (40/60) blend at 200 ^{o}C exhibited the values between the neat

polymers, while EMAA-Na/EB-*g*-MAH (40/60) blend showed higher value than the each component polymer. The data also suggested that there is some kind of attractive interaction between EMAA-Na and EB-*g*-MAH. Moreover, the results agreed well with the results of G_c obtained from ADCB method.

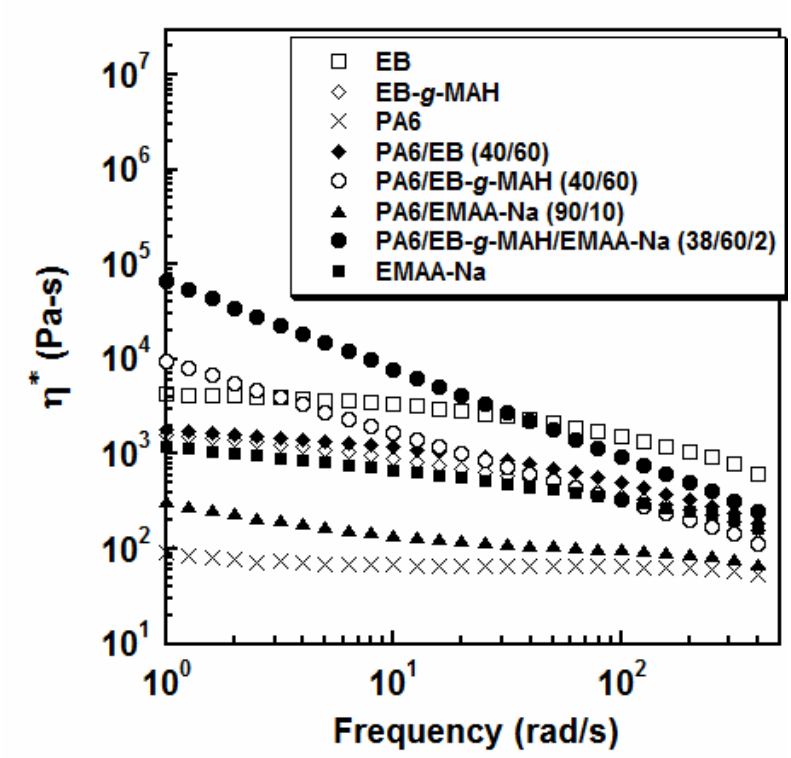

FIGURE 5.5 The complex melt viscosity of neat polymers, binary blends and ternary blends at 250 ^{o}C.

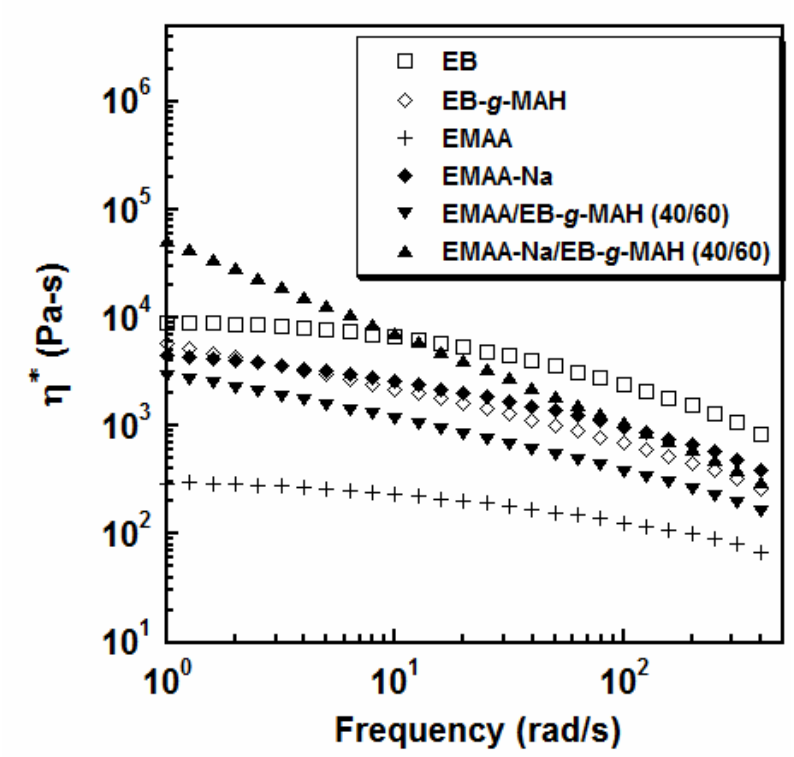

FIGURE 5.6 The complex melt viscosity of neat polymers and binary blends at 200 °C.

To investigate the interactions between the EMAA-Na ionomer and the other component polymers in detail, FT-IR spectra of some blends and the component polymers were measured. FT-IR spectra of EB-*g*-MAH, EMAA, EMAA-NA, PA6, PA6/EB-*g*-MAH, PA6/EB-*g*-MAH/EMAA, and PA6/EB-*g*-MAH/EMAA-Na are shown in Figure 5.7. In the FT-IR spectrum of EB-*g*-MAH, the peak at 1780 cm^{-1} is assigned to the symmetric stretching of cyclic anhydride (1780 cm^{-1}) and the peak at 1710 cm^{-1} is of carboxylic acid resulting from the hydrolysis of the anhydride.[24] The peak at 1780 cm^{-1} was also observed in PA6/EB-*g*-MAH and PA6/EB-*g*-MAH/EMAA

blends, while the peak at 1710 cm^{-1} was overlapped with the rim of the band centered at 1646 cm^{-1} of C=O stretching vibration in PA6. It is thought that the peak of 1780 cm^{-1} in the blends came from EB-*g*-MAH domain in the blend. In contrast to the PA6/EB-*g*-MAH and PA6/EB-*g*-MAH/EMAA blends, the peak was not observed in PA6/EB-*g*-MAH/EMAA-Na blend, even though the morphology of the blend was similar with PA6/EB-*g*-MAH and also had EB-*g*-MAH dispersed phase. To check whether the disappearance of the peak originated in addition of EMAA-Na, FT-IR spectrum of EMAA-Na/EB-*g*-MAH (50/50) was measured as shown in Figure 5.8, and those of EMAA/EB (50/50) and EMAA/EB-*g*-MAH (50/50) were also shown in the figure as the samples for comparison. As the result, the C=O peak of EB-*g*-MAH at 1780 cm^{-1} was not also observed in EMAA-Na/EB-*g*-MAH, while did in EMAA/EB-*g*-MAH. In EMAA-Na/EB-*g*-MAH, Peak in the region from 1500 to 1650 cm^{-1} corresponded to asymmetric stretching vibration region of carboxylate group (COO^-) of EMAA-Na.[25] Figure 5.9 is TEM images of EMAA/EB-*g*-MAH and EMAA-Na/EB-*g*-MAH blends. Both the blends were immiscible and showed the phase separated morphologies, and the morphology of the latter was finer than the former, that is, the compatibility of the EMAA-Na/EB-*g*-MAH blend was much higher than EMAA/EB-*g*-MAH. By the comparison of the two blends, it was suggested that the sodium ion improved the compatibility between EMAA ionomer and EB-*g*-MAH. The disappearance of C=O peak at 1780 cm^{-1} in both blends of PA6/EB-*g*-MAH/EMAA-Na and EMAA-Na/EB-*g*-

MAH meant that the ring-opening of maleic anhydride in EB-*g*-MAH practically occurred by existence of the sodium ion. Neutralization of maleic anhydride by metalcation and disappearance of the peak at 1780 cm^{-1} in PP-*g*-MAH have been reported.[18,19] Therefore, it was expected that the neutralization of anhydride in EB-*g*-MAH by the sodium ion also occurred in the blends. It was reported that the sodium ion in EMAA ionomer can coordinate with two carboxyl groups.[26] In the EMAA ionomer, acid groups preferentially associate with ionic aggregates, and protons and sodium ions can change the coordinating groups each other by acid-cation exchange mechanism.[26] Scheme 5.2 is shown to explain Na^+ ion exchange mechanism of ionomer contained Na^+ ion. It was considered that the ionic aggregates also formed in the neutralized EB-*g*-MAH and then the aggregates acted as physical Crosslinking points in EB-*g*-MAH phase.

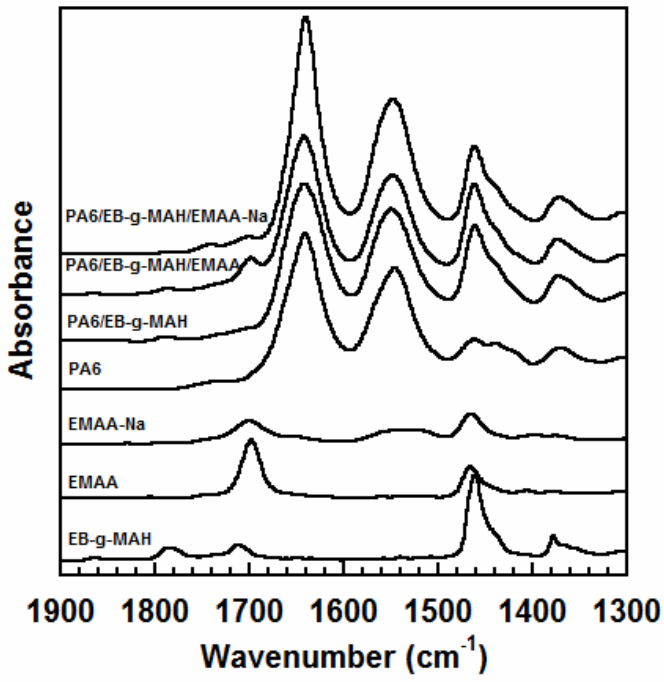

FIGURE 5.7 FTIR spectra of PA6 based blends and component polymers.

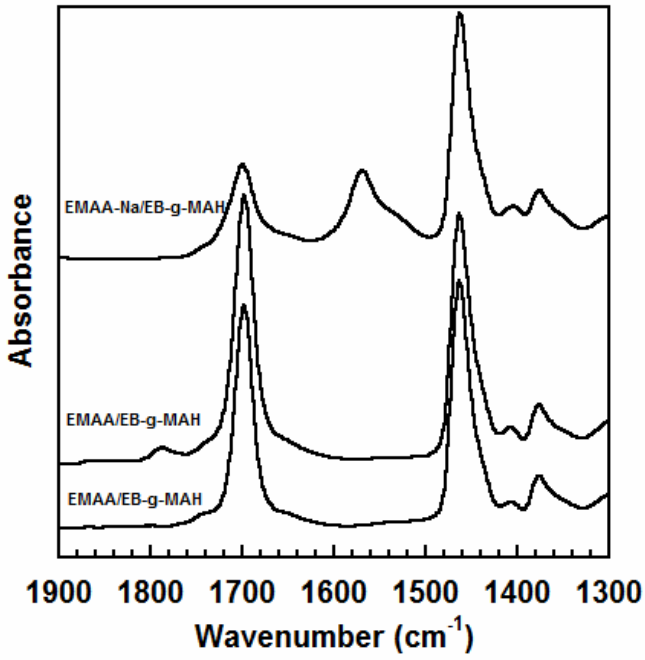

FIGURE 5.8 FTIR spectra of EMAA-Na/EB-*g*-MAH, EMAA/EB and EMAA/EB-*g*-MAH blends.

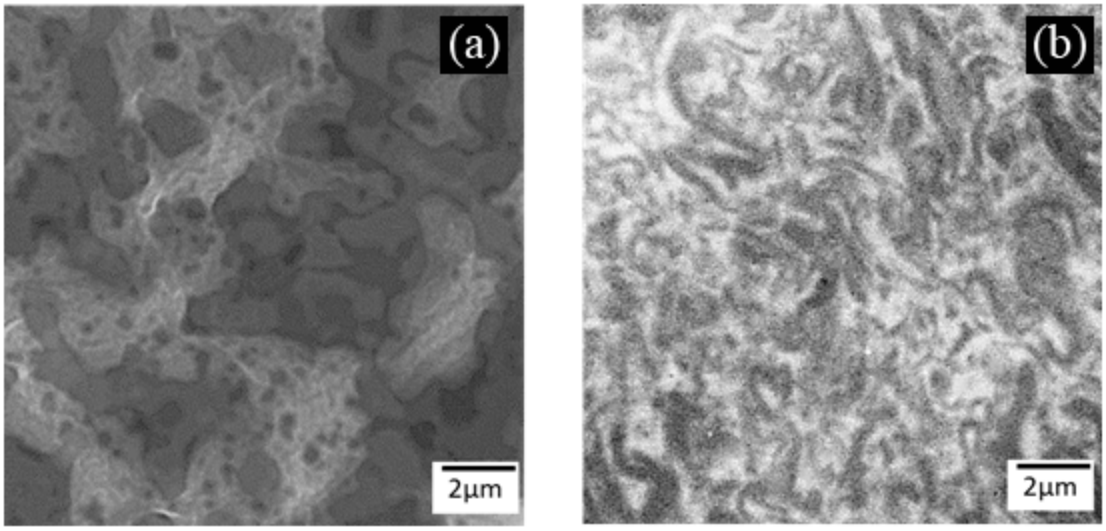

FIGURE 5.9 TEM images of (a) EMAA/EB-*g*-MAH and (b) EMAA-Na/EB-*g*-MAH blends.

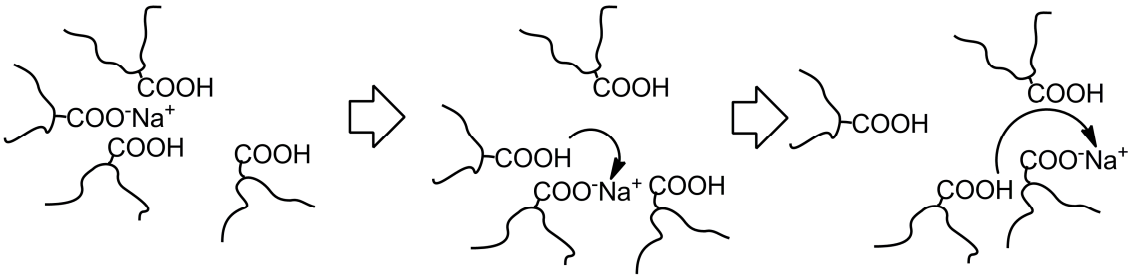

SCHEME 5.2 Na^+ ion exchange mechanism of ionomer neutralized by Na^+ ion.

On the basis of all above results, the model to explain the phase morphology of PA6/EB-*g*-MAH/EMAA-Na blend was proposed as shown in Fig 5.10. It was expected that formation of the ionic aggregates were not only formed in EMAA-Na ionomer but

also in EB-*g*-MAH by both sodium ion and acid groups. The ionic aggregates acted as physical crosslinking point in the blended phase of EMAA-Na and EB-*g*-MAH rubber, and the physical crosslinking must improve the mechanical properties of PA6/EB-*g*-MAH/EMAA-Na blend.

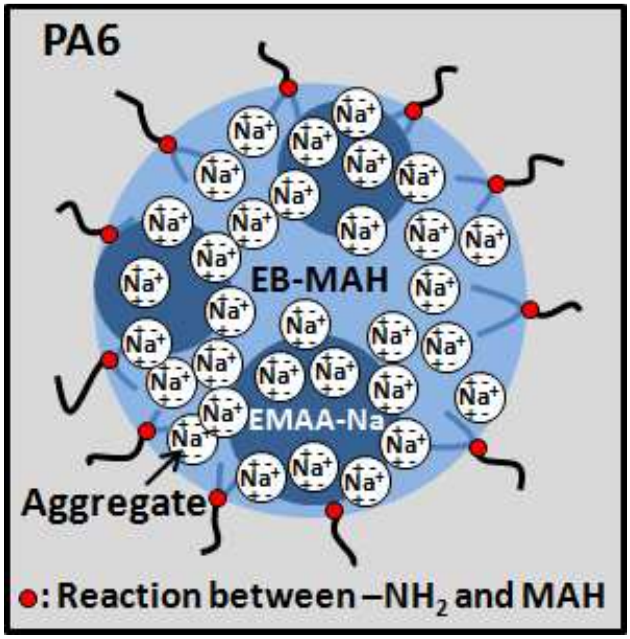

SCHEME 5.10 Schematic illustration of phase morphology of PA6/EB-*g*-MAH/EMAA-Na blend.

5.4 CONCLUSIONS

New TPE was successfully developed by blending PA6, EB-*g*-MAH and EMAA-Na. Elongation at break and elastic recovery were improved by MAH, while

tensile strength at break increased by addition of EMAA-Na. Morphology of PA6/EB and PA6/EB-*g*-MAH was completely different, that is, EB-*g*-MAH was the dispersed phase in PA6/EB-*g*-MAH because of the interfacial reaction, while EB, which was major component in PA6/EB, constituted the matrix phase. By addition of small amount of EMAA-Na ionomer to PA6/EB-*g*-MAH blend, the tensile modulus increased. EMAA-Na was expected to locate inside EB-*g*-MAH due to higher interfacial adhesion of EMAA-Na/EB-*g*-MAH than EMAA-Na/PA6 and the fine morphology of EMAA-Na/EB-*g*-MAH blend. From the FT-IR measurement which showed disappearance of anhydride ring of EB-*g*-MAH, it was expected that ionic aggregates were formed in EB-*g*-MAH phase by the sodium ion. The improvement in mechanical properties can be explained by the ionic aggregates formation which acts as physical crosslinking points in the rubber phase.

5.5 REFERENCES

1. Sharpc, L. H. *J. Adhesion,* **1989**, 29, 1.
2. Fernandez-Garcia, J. G.; Orgiles-Barcelo, A. C.; Martin-Martinez, J. M. *J. Adhesion Sci. Technol.*, **1991**, 5, 1065.
3. Li, Y.; Oono, Y.; Kadowaki, Y.; Inoue, T.; Nakayama, K.; Shimizu, H. *Macromolecules* **2006**, 39, 4195.
4. Jha, A.; Bhowmick, A. k. *Rubber Chem. Technol*., **1997**, 70, 798.

5. Jha, A.; Bhowmick, A. k.; Fujitsuka, R.; Inoue, T. *J. Adhesion Sci. Technol*., **1999**, 13, 649.
6. Ho,C. H.; Wang, C. H.; Lin, C. I.; Lee, Y. D. *Polymer*, **2008**, 49,3902.
7. Stagnaro, S. P.; Cai, C. L.; Yin, J. H.; Costa, G.; A. Turturro, A. *J. Appl. Polym. Sci.*, **2008**, 110, 3963.
8. Ohishi, H. *J.Appl. Polym. Sci.* **2004**, 93, 1567.
9. Antony, P.; Bandyopadhyay, S.; De, S.K. *J. Mater. Sci.* **1999**, 34, 2553.
10. Datta, S.; De, P.P.; De, S.K. *J. Appl. Polym. Sci.* **1996**, 61, 1839.
11. Abad, M.J.; Ares, A.; Barral, L.; Cano, J.; Diez, F.J.; Garcia-Garabal, S.; Lopez, J.; Ramirez, C. *J Appl. Polym. Sci.* **2004**, 94, 1763.
12. Jha, A.; Bhowmick, A. k. *Polymer* **1996**, 38, 4337.
13. Coran, A.Y.; in Handbook of Elastomer-New Developments and Technology. Marcel Dekker, Inc., New York, **1988**, pp. 249.
14. Koriyama, H.; Oyama, H. T.; Ougizawa, T.; Inoue, T.; Weber, M.; Koch, E., *Polymer*, **1999**, 40, 6381.
15. Kumar, S.; Ramanaiah, B. V.; Maiti, S. N. *Soft Matter.*, **2007**, 4(1), 85.
16. Shashidhara, G. M.; Biswas, D.; Pai, B. S.; Kadiyala, A. K.; Feroze, G. S. W.; Ganesh, M., *Polym. Bull*., **2009**, 63, 147.
17. Zhou, Y.; Wang, W.; Dou, R.; Li, L. P.; Yin, B.; Yang, M. B., *Polym. Eng. Sci*., **2012**, DOI: 10.1002/pen.23445.

18. Antony, P.; Battacharya, A.K; De, S.K., *J. Appl. Polym. Sci.*, **1999**, 71, 1257.

19. Rousseaux, D. D. J.; Sclavons, M.; Godard, P.; Brynaert, J. M. *Polym. Degrad. Stabil*. **2010**, 95, 1194.

20. Charoensirisomboon, P.; Chiba, T.; Inoue, T.; Weber, M. *Polymer* **2000**, 41, 5977.

21. Ide, F.; Hasegawa, A. *J. Appl. Polym. Sci.***1974**, 18, 963.

22. Roeder, J.; Oliveira, R.V.B.; Goncalves, M.C.; Soldi, V.; Pires, A.T.N. *Polym. Test.***2002**, 21, 815.

23. Zhou, X.; Zhang, P.; Jiang, X.; Rao, G. *Vib. Spectrosc*. **2009**, 49, 17.

24. Barra, G. M. O.;Crespo, J. S.;Bertolino, J. R.;Soldi, V;Pires, A. T. N., *J. Braz. Chem*. **1999**, 10, 31.

25. Kutsumizu, S.; Hara, H.; Tachino, H.; Shimabayashi, K.; Yano, S. *Macromolecules* 1999, 32, 6340-6347.

26. Nishio, M.; Nishioka, A.; Taniguchi, T; Koyama, K. *Polymer*, **2005,** 46, 261.

CHAPTER 6

General Conclusions

Thermoplastic elastomers (TPEs) have attracted extensive attention from polymer technology developers and scientists, because TPEs behave like elastic-rubber at low temperature and melt-processable at elevated temperatures, while crosslinked rubber material does not flow. Therefore, TPEs have been developed for various applications such as automotive, electrical and medical ones. In the recent years, the environmental friendly and renewability of the biodegradable plastics have motivated some researchers to develop the biodegradable TPEs. Moreover, high performance TPEs have been also investigated so far. To obtain the blend with excellent mechanical properties and elasticity by polymer blending, it is necessary to control the blend morphology and the adhesion between the component polymers in an immiscible polymer blend, which has been one of the most important longtime issues.

In this thesis, new types of TPEs were developed by using different techniques of polymer blending, and their morphology, properties and reaction were investigated to find the relationship.

In Chapter 2, poly(butylene succinate) (PBS) was blended with ethylene-propylene-diene terpolymer (EPDM) and ethylene-1-butene copolymer (EB), which maleic anhydride (MAH) was grafted on both rubbers. Both blends showed excellent tensile and elastic properties, and they elongated and recovered similar to crosslinked rubbers.PBS/EB-MAH blend showed the better strain recovery because of the increased interfacial crosslink, the presence of small rubber particle and the better elasticity of EB rubber. To improve the poor interfacial adhesion because of low reactivity of MAH with end groups of PBS, the samples were annealed at 170 ^{o}C to progress the reaction at the interface. Tensile strength and elongation at break were improved by the annealing. It was found that the annealing was very effective to improve the interfacial adhesion through the reaction between the PBS terminal groups and the MAH group of the rubbers, and also promoted cross-linking of EPDM rubber.

In Chapter 3, PBS was blended with acrylic rubber (ACM) by two methods. First, dicumyl peroxide (DCP) was directly added during mixing. Second, ACM had pre-grafted with poly[methylene (phenylene isocyanate)] (PMPI) before mixed with PBS.PBS/ACM/DCP blend presented smaller particle size, good dispersion, higher elongation at break, better tensile strength and recovery like rubber compared to PBS/ACM-PMPI blend. These were due to the increasing of interfacial reaction, which improved compatibility and properties of the blend. Therefore, it was indicated that DCP was more efficient in compatibilizing the PBS/ACM blend.

In Chapter 4, poly(lactic acid) (PLA) was blended with ACM and ethylene-methacrylic acid ionomer with sodium ion (EMAA-Na).Elastic recovery of PLA/ACM was improved by addition of EMAA-Na, while morphology of PLA/ACM/EMAA-Na

was almost the same with PLA/ACM and PLA/ACM/EMAA. Maldistribution of EMAA-Na in ACM phase was observed. The results of viscosity and FT-IR data indicated that Na^+ ion in EMAA-Na increased interfacial reaction between end group of PLA and epoxy group of ACM, because Na^+ ion acted as a catalyst to accelerate the reaction. High crosslinking density by addition of 4 phr of hexamethylene diamine carbamate (HMDC) was found to change morphology of PLA/ACM/EMAA-Na blend from co-continuous morphology to the connecting morphology of ACM particles in PLA matrix, and the EMAA-Na was still observed in ACM phase. The EMAA-Na inside ACM phase was expected to form some chemical and physical crosslinking, and then they formed some network of rubber particles. It was indicated that the increasing of interfacial reaction by Na^+ ion as a catalyst and the mechanical properties of the PLA/ACM/EMAA-Na blend was improved by high crosslinking density inside ACM phase by addition of high amount of HMDC cross-linking agent and resultant morphology change.

In Chapter 5, the effect of EMAA-Na on polyamide (PA6) blended with EB-MAH was investigated. In the PA6/EB-MAH blend, increasing of interfacial adhesion was suggested to the reaction between amino end groups of PA6 with MAH groups of EB-*g*-MAH. EMAA-Na was expected to locate inside EB-*g*-MAH, and formed ionic aggregates. From the FT-IR measurement, it was suggested that MAH ring in EB-*g*-MAH opened by Na^+ ion. TEM image of the PA6/EB-*g*-MAH/EMAA-Na blend and the improved tensile properties suggested ionic aggregates were formed in the rubber phase and they acted as physical crosslinking points inside the EB-*g*-MAH rubber phase. In this study, it was indicated that the physical crosslinking points, which is ionic

aggregates, can be introduced to a maleic anhydride grafted polymer by addition of EMAA-Na and improved the mechanical properties of the blend

In these investigations, we successfully developed new TPEs made by the biodegradable plastics and polyamide with excellent properties. These TPEs might be useful for some application of industrial elastic materials. However, it is considered that the concept of biodegradable TPEs and the effect of ionomer in polymer blending open the way towards further development of polymer materials. We expected that the information obtained in this investigation will be helpful for better understanding of the TPEs development.

Acknowledgements

First, I would like to thank my advisor, Professor Toshiaki Ougizawa, who's accepting me as his student, encouragement, guidance and support from the initial to the final level enabled me to develop an understanding of the subject.

I am deeply grateful to Dr. Keiichi Kuboyama, for his constant assistant in helping with the instrument, providing fruitful and constructive discussions contributed tremendously to our research.

I have been very lucky throughout most of my life in graduate school of Tokyo Institute of Technology, in that I have been able to concentrate mostly on my research. This is due to the supporting scholarship from the Government of Japan (MEXT).

I have also been fortunate to have many great groups of friends at Tokyo Tech. These include all members of the Ougizawa laboratory, THAI students and many other students. I would like to thank all in the instrument training, encouragement and group discussions. The groups have been a source of friendships as well as good advice and collaboration.

Lastly, I offer my regards and blessings to all of those who supported me in any respect during the completion of the research at Tokyo Institute of Technology.

Tokyo Institute of Technology

September 2013

Kittisak Jantanasakulwong